Programmable epigenome editing by transient delivery of CRISPR epigenome editor ribonucleoproteins

Da Xu[1,8], Swen Besselink[1,2,8], Gokul N. Ramadoss[3], Philip H. Dierks[3], Justin P. Lubin[4], Rithu K. Pattali[1], Jinna I. Brim[1], Anna E. Christenson[1], Peter J. Colias[1], Izaiah J. Ornelas[1], Carolyn D. Nguyen[1], Sarah E. Chasins[4,5], Bruce R. Conklin[3,6,7], James K. Nuñez[1,5]

Author Affiliations

[1] Department of Molecular and Cell Biology, University of California, Berkeley, CA, 94720, USA.
[2] Molecular Mechanisms of Disease Master's Program, Radboud University, Nijmegen, 6525EZ, the Netherlands.
[3] Gladstone Institutes, San Francisco, CA, 94158, USA.
[4] Department of Electrical Engineering and Computer Sciences, University of California, Berkeley, CA, 94720, USA.
[5] Chan Zuckerberg Biohub - San Francisco, CA, 94158, USA.
[6] Department of Cellular and Molecular Pharmacology, University of California, San Francisco, CA, 94158, USA.
[7] Department of Medicine, University of California, San Francisco, CA, 94158, USA.
[8]These authors contributed equally: Da Xu, Swen Besselink.

Corresponding author: jamesnunez@berkeley.edu

Abstract

Programmable epigenome editors modify gene expression in mammalian cells by altering the local chromatin environment at target loci without inducing DNA breaks. However, the large size of CRISPR-based epigenome editors poses a challenge to their broad use in biomedical research and as future therapies. Here, we present Robust ENveloped Delivery of Epigenome-editor Ribonucleoproteins (RENDER) for transiently delivering programmable epigenetic repressors (CRISPRi, DNMT3A-3L-dCas9, CRISPRoff) and activator (TET1-dCas9) as ribonucleoprotein complexes into human cells to modulate gene expression. After rational engineering, we show that RENDER induces durable epigenetic silencing of endogenous genes across various human cell types, including primary T cells. Additionally, we apply RENDER to epigenetically repress endogenous genes in human stem cell-derived neurons, including the reduction of the neurodegenerative disease associated V337M-mutated Tau protein. Together, our RENDER platform advances the delivery of CRISPR-based epigenome editors into human cells, broadening the use of epigenome editing in fundamental research and therapeutic applications.

Introduction

Advances in genome and epigenome editing have greatly broadened the ability to manipulate human cells, fueling both fundamental research and therapeutic applications[1–3]. Epigenome editing represents an attractive approach for regulating gene expression without inducing potentially harmful DNA breaks or permanently changing the underlying genome sequence[4–14]. Instead, programmable transcriptional repression or activation is induced by altering epigenetic modifications on DNA and histones, typically by epigenome editing tools that consist of epigenetic effector domains derived from transcriptional repressors and activators that are synthetically coupled to programmable DNA-binding proteins such as zinc finger (ZF), transcription activator-like effector (TALE) or catalytically deactivated Cas (dCas) proteins[15].

Recent developments in epigenome editing include methods to program durable epigenetic repression of endogenous mammalian genes by transient expression of synthetic epigenetic repressors that simultaneously establish *de novo* DNA methylation and repressive H3K9me3 at target gene promoters[16,17]. Such programmable hit-and-run epigenome editing tools combine the DNMT3A-DNMT3L (DNMT3A-3L) enzymatic complex to catalyze *de novo* DNA methylation and the Krüppel-associated box (KRAB) transcriptional repressor domain that recruits cofactors to deposit H3K9me3. Recently, ZF- and TALE-based hit-and-run epigenome editors have been applied in mouse models to durably repress *Pcsk9* in the liver and a prion gene in the brain[18,19]. While these approaches highlight the potential for *in vivo* therapeutic epigenome editing, the reliance on ZF and TALE DNA-binding platforms restricts multiplexing and easily programmable capabilities offered by RNA-guided CRISPR-dCas9.

Previously, we engineered the CRISPRoff epigenome editor by synthetically fusing dCas9 to DNMT3A-3L and KRAB epigenetic effector domains for programmable multiplexed durable gene silencing across various cell types and for pooled genome-wide screens[16]. However, the large size of CRISPR-based epigenome editors, including CRISPRoff, poses a significant barrier to their efficient delivery into human cells, thereby limiting their broader use. For example, CRISPRoff (~7.2 kilobase pairs) exceeds the packaging capacity of adeno-associated virus (AAV) delivery vectors and prolonged AAV expression of epigenome editors may increase the risk of off-target editing[3,20]. Additionally, mRNA-based delivery of CRISPR reagents requires electroporation that is potentially cytotoxic or as lipid nanoparticle (LNP)-mRNA complexes that require cell type-specific formulation that remains a current challenge[21–23].

Alternatively, delivering CRISPR reagents as ribonucleoprotein (RNP) complexes offers multiple benefits[22–24]. First, RNP delivery does not require transgene or viral vector-based expression, thus there is no potential risk of viral DNA integration. Second, RNP is the most transient delivery formulation of CRISPR editors, thereby minimizing exposure time in target cells and decreasing off-target editing. However, many commonly used epigenetic effectors, such as KRAB and MeCP2, contain intrinsically unstructured regions that are challenging to purify *in vitro* for RNP delivery methods[25,26]. Thus, there is an unmet need for a platform to transiently deliver CRISPR epigenome editors as RNPs into mammalian cells for modulating gene expression.

Virus-like particles (VLPs), or enveloped delivery vehicles (EDVs), derived from retroviruses such as the murine leukemia virus or human immunodeficiency virus, have emerged recently as efficient vehicles for transient CRISPR-based genome editors delivery as RNP complexes[27–34]. VLPs provide several unique advantages over other delivery methods for CRISPR technologies. First, VLPs are less limited by cargo size, making them well-suited to deliver large CRISPR cargos. Second, VLPs are composed of viral proteins that encapsulate their cargo in a protective shell and possess the natural ability to enter cells, but lack viral genetic material, thereby eliminating the risk of viral genome integration[35]. As such, VLP-based delivery has been adapted for CRISPR nucleases, base editors, and prime editors, highlighting the diverse cargo payload of VLPs[27–31]. To our knowledge, VLPs have not been explored yet for RNP delivery of CRISPR epigenome editors.

Here, we leverage engineered virus-like particles to transiently deliver various CRISPR epigenome editor RNPs for programmable gene silencing and activation in human cells. We term our platform RENDER, Robust ENveloped Delivery of Epigenome-editor Ribonucleoproteins. We apply RENDER for efficient epigenetic silencing of endogenous genes that persists for weeks and is broadly applicable across various human cell types, including donor-derived primary T cells. We demonstrate that RENDER-based delivery of CRISPRoff into induced pluripotent stem cell-derived neurons results in durable repression of the V337M-mutated *MAPT* gene, thereby reducing protein levels of the neurodegenerative disease associated Tau protein. We envision our RENDER platform for transient delivery of CRISPR epigenome editors to advance the broad use of programmable epigenome editing in biomedical research and therapeutic applications.

Results

eVLPs enable delivery of various epigenome editor RNP into human cells

Previously, the murine leukemia virus has been engineered for VLP delivery of Cas9 nuclease, base editor (BE), and prime editor[30,31]. We hypothesized that these engineered virus-like particles (eVLPs) could also be adapted to deliver epigenome editors as RNP complexes (**Fig. 1a**). To test this, we modified the BE-eVLP platform by substituting the base editor in the gag-editor fusion protein with various epigenome editors, including CRISPRi, DNMT3A-3L-dCas9 and CRISPRoff (**Fig. 1b**). Furthermore, as several studies have reported improved epigenetic silencing with the ZIM3 KRAB domain compared to the widely-used KOX1 KRAB domain, we aimed to directly compare the two KRAB domains for CRISPRi and CRISPRoff in the eVLP delivery system[36,37]. As control, we used dCas9 with no epigenetic effector domain fused. Epigenome editor eVLPs were produced by co-transfecting Lenti-X HEK293T cells with plasmids encoding the envelope protein VSV-G, wild-type gag-pol polyprotein, gag-epigenome editor fusion protein, and single-guide RNA (sgRNA) (**Fig. 1a**). Three days post-transfection, we collected the supernatant containing the eVLPs and concentrated the virus-like particles. Western blot analysis of concentrated CRISPRoff-eVLPs confirmed successful packaging of CRISPRoff proteins in the eVLP as pre- and post-cleavage species from the gag-CRISPRoff fusion protein (**Fig. 1c**).

To assess whether eVLPs can deliver functional epigenome editors into cells, we co-packaged eVLPs with each epigenome editor and a sgRNA targeting the *CLTA* promoter. Subsequently,

actively dividing HEK293T cells that stably express an endogenous GFP-tagged *CLTA* gene were treated with a single dose of the different epigenome editor eVLPs (**Fig. 1d**). Successful epigenetic silencing is signified by a reduced CLTA-GFP protein expression, which can be measured quantitatively in single cells using flow cytometry. Three days post-treatment, we observed varying levels of CLTA-GFP silencing by the different epigenome editor eVLPs, with dCas9-eVLPs showing only modest CLTA-GFP repression in 25% of the treated cells (**Fig. 1e**). Remarkably, eVLPs packaged with CRISPRi, DNMT3A-3L-dCas9 or CRISPRoff induce robust epigenetic silencing, resulting in over 75% of treated cells with CLTA-GFP silenced (**Fig. 1e**, **1f**, and **Extended Data Fig. 1a**). Furthermore, the ZIM3 KRAB domain induces higher epigenetic silencing compared to KOX1 within the CRISPRi-eVLPs, whereas both KRAB domains show comparable silencing efficiency within CRISPRoff (**Extended Data Fig. 1b** and **1c**).

Then, we monitored the durability of epigenetic silencing over 14 days after a single dose of our different epigenome editor eVLPs. Cells treated with dCas9-eVLPs or CRISPRi-eVLPs fully reactivate CLTA-GFP expression to pre-treatment levels after 7 days, consistent with the transient epigenetic silencing activity of CRISPRi (**Fig. 1g** and **Extended Data Fig. 1d**). In contrast, cells treated with DNMT3A-3L-dCas9-eVLPs or CRISPRoff-eVLPs maintain robust epigenetic silencing due to the heritability of the programmed DNA methylation at the *CLTA* promoter as we have shown previously[38] (**Fig. 1g**). Together, these findings demonstrate that the eVLP platform can effectively package and deliver functional epigenome editor RNPs into human cells to induce transient repression (CRISPRi) or durable epigenetic silencing (DNMT3A-3L-dCas9, CRISPRoff). We refer to our eVLP-mediated packaging and delivery of CRISPR epigenome editors as RENDER, Robust ENveloped Delivery of Epigenome-editor Ribonucleoproteins.

Reversible epigenome editing by RENDER-TET1-dCas9

An advantage of epigenome editing is the reversibility of the programmed epigenetic modifications at target loci[16]. We next applied RENDER to deliver the TET1-dCas9 (v4) epigenome editor that can enzymatically remove repressive DNA methylation from target gene promoters to activate gene transcription[16]. We packaged TET1-dCas9 in eVLPs and treated actively dividing HEK293T cells in which CLTA-GFP has been durable repressed by CRISPRoff (**Fig. 1h**). Compared to untreated cells, we observe increased CLTA-GFP expression in ~6% of cells at 6 days post-treatment that remains stable for 15 days (**Fig. 1i** and **1j**). We envision that further engineering will improve the reactivation efficiency of RENDER-TET1-dCas9, including co-packaging with transcriptional activator domains to recruit the transcriptional machinery, as we have shown previously with CRISPRon[16].

Rational optimization of RENDER-CRISPRoff

An advantage of virus-like particle delivery platforms is the ability to perform dose-dependent treatments to titrate the amount of editors delivered into cells. Indeed, varying the dose with our RENDER platform results in titratable degrees of CLTA-GFP silencing in HEK293T cells for each epigenome editor repressor we tested (**Fig. 2a**, **2b** and **Extended Data Fig 2a-d**). Noticeably, we observed that lower doses of RENDER-CRISPRoff result in weaker durability of gene silencing over a 14-day time course (**Fig. 2a**). Given that the eVLP delivery platform was optimized initially

for CRISPR base editors that differ in size and biochemical properties from epigenome editors, we sought to refine the RENDER platform tailored specifically for CRISPRoff (ZIM3) (**Fig. 2c**).

First, we hypothesized that optimizing the cargo-to-vector ratio will increase the amount of CRISPRoff RNPs within the eVLPs, thereby improving the efficacy of epigenetic silencing. While keeping the amounts of other plasmids constant, we varied the ratio of gag-CRISPRoff to gag-pol plasmids during co-transfection to package CRISPRoff-eVLPs. Intriguingly, we found that eVLPs can accommodate a high proportion of CRISPRoff, with a 90:10 ratio of gag-CRISPRoff to gag-pol plasmids achieving the most effective gene silencing (**Fig. 2d**). This formulation – demonstrating 99% silencing at maximum dose and a 3.9-fold improved potency (EC50) – is termed RENDER-CRISPRoff v2 (**Extended Data Fig. 3a**).

Next, we hypothesized that an increased number of CRISPRoff proteins within the eVLP will necessitate additional sgRNA to form functional RNP complexes. Thus, we titrated the amount of sgRNA plasmids in our plasmid transfections for CRISPRoff-eVLP packaging. Our results show that increasing the amount of sgRNA further improves the editing efficiency at non-saturating doses, yielding RENDER-CRISPRoff v3 (**Fig. 2e** and **Extended Data Fig. 3b**). These findings demonstrate that by optimizing the component ratios of CRISPRoff-eVLPs, we improve its potency by 4.4-fold compared to v1, thereby lowering the dose required to achieve efficient target gene silencing (**Fig. 2f**). A single dose of the optimized RENDER-CRISPRoff v3 induces highly efficient and durable gene silencing, with 92% of cells maintaining stable repression of CLTA-GFP at 49 days post-treatment (**Fig. 2g** and **2h**). To confirm that the optimized RENDER-CRISPRoff v3 can achieve durable silencing across different target genes, we further evaluated its performance in HEK293T cells expressing an endogenous GFP-tagged *H2B* gene, which resulted in durable silencing in 99% of cells at 29 days post-treatment (**Fig. 2i**).

RENDER-CRISPRoff editing across various human cell types

After optimization in HEK293T reporter cells, we aimed to evaluate the broad applicability of RENDER-CRISPRoff across eight human cell lines originating from different tissues: embryonic kidney (HEK293T), liver (HepG2), leukemic T cells (Jurkat), retinal epithelium (hTERT RPE-1), glioblastoma (U87 MG), lymphoblast (K562), cervical cancer (HeLa), and neuroblastoma (SH-SY5Y) cells. We packaged CRISPRoff with sgRNAs targeting either the promoter of *CD55* or *CD81*, which encode cell surface proteins that are nonessential for cell viability. Seven days post-treatment, we performed antibody staining for CD55 and CD81 to measure gene silencing in single cells using flow cytometry. RENDER-CRISPRoff induces robust silencing of CD55 in HEK293T, HepG2, Jurkat, hTERT RPE-1, and U87 MG cells (>80% silenced), whereas CD81 silencing is efficient in Jurkat, hTERT RPE-1, U87 MG, HeLa, and SH-SY5Y cells (>44% silenced) (**Fig. 3a**). Notably, we observed weaker silencing efficiency for CD81 in HEK293T and CD55 in HeLa, which we hypothesize is not a RENDER limitation, but rather due to differences in gene regulatory landscapes across different cell types as shown previously[39–41]. In contrast, we detect overall lower silencing efficiency in K562 cells (~22%) that is likely due to a cell type-specific virus-like particle delivery limitation. These results demonstrate the versatility and efficiency of the RENDER platform to deliver CRISPRoff in diverse human cell types, underscoring its potential for broader applications.

Global profiling of DNA methylation after RENDER-CRISPRoff treatment

To confirm epigenome editing after RENDER-CRISPRoff treatment, we isolated Jurkat cells 16 days after a single dose of CRISPRoff targeting *CD55* and performed genome-wide DNA methylation profiling with enzymatic methyl sequencing (EM-seq). Our EM-seq data show significant enrichment of DNA methylation at the *CD55* gene after RENDER-CRISPRoff treatment as compared to untreated cells (**Fig. 3b**). DNA methylation enrichment spans a 1.5 kb region at the *CD55* promoter that includes the annotated CpG island (CGI) and extends ~200 bp upstream of the annotated CGI (**Fig. 3c** and **3d**). Additionally, we analyzed the top ten most significant differentially methylated regions in both RENDER-CRISPRoff treated and untreated cells and observed only modest changes in DNA methylation at unintended genomic loci compared to the target *CD55* locus, consistent with our previous DNA methylation profiling after CRISPRoff plasmid expression (**Extended Data Fig. 4** and **5**)[16].

Multiplexed epigenome editing with RENDER

A key advantage of CRISPR platforms is their ability to target multiple genes simultaneously within the same cell. We hypothesized that the RENDER-CRISPRoff platform could similarly enable multiplexed gene silencing, as demonstrated previously with CRISPRoff plasmid transfections[38]. To test this, we packaged CRISPRoff-eVLPs with a pool of plasmids encoding different sgRNAs targeting the promoters of *CD55* and *CD81* and delivered the particles to Jurkat and U87 MG cells (**Fig. 3e**). Seven days post-treatment, both cell lines resulted in a detectable population with both CD55 and CD81 silenced (46% for Jurkat and 82% for U87) (**Fig. 3f** and **3g**). These results further demonstrate the broad use of the RENDER platform in simultaneously targeting multiple genes in a one-shot treatment.

Additionally, we aimed to enhance silencing efficacy by combining multiple sgRNAs that target the same gene promoter. To test this, CRISPRoff-eVLPs were packaged with either individual sgRNAs or a pool of three distinct sgRNAs targeting the same gene promoter. Fourteen days post-treatment in Jurkat cells, we observed improved silencing efficiency for *CD29*, *CD55*, and *CD81* when employing a pool of three sgRNAs in a single CRISPRoff-eVLP (**Extended Data Fig. 3c**). Notably, pooling three sgRNAs targeting *CD81* was effective even when one of the individual sgRNAs displayed minimal activity. Together, these findings underscore the use of multiplexed RENDER to enhance target gene silencing efficiency, particularly in cases where individual sgRNAs demonstrate suboptimal activity, reinforcing its versatility for complex gene silencing applications.

Large-scale and CRISPRoff apoprotein delivery

To evaluate whether RENDER could be applied for large-scale cell engineering, we assessed its performance across large cell populations. First, we delivered CRISPRoff to a population of 1.0×10^6 HEK293T cells at once, achieving over 92% silencing efficiency of CLTA-GFP, consistent with the silencing efficiency from our small-scale experiments using 1.5×10^4 cells (**Fig 3h**). Furthermore, we optimized RENDER transduction for suspension cells and achieved over 96% silencing of CD55 and CD81 after CRISPRoff delivery to 5.0×10^5 Jurkat cells at once, expanding from the initial 1.5×10^4 cells tested previously (**Fig 3i**, **Extended Data Fig 3d** and **3e**).

Additionally, we hypothesized that RENDER could facilitate transient delivery of epigenome editor as apo-form proteins that assemble with sgRNAs within the target cell to form functional RNP complexes. We packaged CRISPRoff protein without sgRNA and treated CLTA-GFP HEK293T cells that constitutively express a sgRNA targeting the *CLTA* promoter (**Fig. 3j**). At four days post-treatment, we observe a silencing efficiency of ~93% at the highest dose, indicating successful CRISPRoff apoprotein delivery and RNP assembly within the sgRNA-expressing cells (**Fig. 3k**). Together, these results highlight the scalability of RENDER for applications in cell engineering and future use in high-throughput CRISPR screening where large cell quantities are required.

Epigenome editing in primary human T cells with RENDER-CRISPRoff

T cells are used widely in cancer immunotherapy and frequently engineered using Cas9 nucleases to disrupt inhibitory genes. However, Cas9-mediated genome editing in T cells has been associated with adverse outcomes, including chromosomal deletions, truncations, and translocations[11]. Furthermore, delivery of genome editing reagents relies predominantly on electroporation of reagents, which requires dedicated hardware and introduces substantial cytotoxicity, elevated costs, and manufacturing burdens within cell therapy protocols[23,24,42–44].

To explore the application of RENDER-CRISPRoff in primary T cell engineering, we compared its performance against CRISPRoff-encoded mRNA electroporation. Naïve T cells were first isolated from peripheral blood mononuclear cells of a healthy donor and activated for two days. The activated T cells were then either treated with a single dose of RENDER-CRISPRoff targeting the *CD55* promoter or with a non-targeting control sgRNA, or electroporated with CRISPRoff mRNA and sgRNA (**Fig. 4a**). By two days post-treatment, we observe that RENDER-CRISPRoff treated T cells are more viable than electroporated T cells, with ~75% viability compared to ~42%, respectively (**Fig. 4b** and **4c**). Eleven days post-treatment, CD55 is silenced in 21% of RENDER-treated T cells, while 97% of mRNA-electroporated T cells were silenced (**Fig. 4d** and **4e**). Similarly, we compared silencing efficiency for CD81 and observed that CD81 is silenced in 35% of the T cells treated with RENDER-CRISPRoff targeting CD81, compared to 78% for mRNA-electroporated T cells (**Fig. 4f**). These findings establish RENDER as a promising approach to engineer primary T cells through epigenome editing with minimal effects on cell viability as compared to mRNA electroporation.

Therapeutic epigenome editing in iPSC-derived neurons

Many neurodegenerative diseases are caused by the toxic accumulation of mutant proteins, positioning them as attractive candidates for therapeutic genome editing aimed at perturbing the underlying mutated genes. However, conventional genome editing in neurons is challenging due to unique mechanisms in DNA double-strand break (DSB) repair[45]. A single treatment that could robustly and durably silence disease-associated genes in neurons without inducing DSBs, would offer a powerful alternative for therapeutic intervention.

To generate programmed epigenetic repression of endogenous genes in neurons, we previously transfected plasmid DNA expressing CRISPRoff into induced pluripotent stem cells (iPSCs), followed by neuronal differentiation. The efficacy of RENDER across diverse cell types motivated

us to test the delivery of epigenome editor RNPs directly into neurons to repress endogenous genes, thereby bypassing the requirement of pre-editing in iPSCs. We first packaged CRISPRoff with sgRNAs targeting the *CD81* promoter and treated neurons 10 days post-differentiation from WTC-11 iPSCs (**Fig. 5a**). Seven days post treatment, we observe robust silencing of CD81 in treated neurons, with a 79% reduction in total CD81 protein levels compared to the non-targeting control (**Fig. 5b** and **5c**). To test the durability of epigenetic repression in neurons, we also measured CD81 levels two weeks after CRISPRoff treatment and observed that CD81 remains stably repressed in the majority of treated neurons (**Fig. 5b** and **5c**). These results demonstrate that RENDER mediates robust target gene repression in iPSC-derived neurons, thereby enabling us to engineer customized neurons with target genes repressed durably.

Silencing of the gene *MAPT*, which encodes Tau protein, is of great therapeutic interest for treating neurodegenerative diseases. Studies have shown that reducing *MAPT* expression protects against cognitive deficits in Alzheimer's disease model mice[46]. Additionally, *MAPT* missense mutations directly contribute to tauopathies, such as the V337M mutation that is associated with frontotemporal dementia (FTD). Current therapeutic strategies, including small interfering RNA (siRNA), antisense oligonucleotides (ASOs), and antibodies, require regular re-dosing to maintain efficacy. In contrast, the RENDER platform offers a promising approach to achieve durable repression of Tau expression with a single treatment. To investigate the potential therapeutic use of RENDER in neuronal contexts, we delivered CRISPRoff with sgRNAs targeting the *MAPT* promoter in iPSC-derived neurons harboring the *MAPT* V337M mutation (**Fig. 5a**). Eight days post-treatment with a high dose of CRISPRoff, we observed an approximate 63% reduction in Tau protein expression in the treated neurons, compared to non-targeting control (**Fig. 5d** and **5e**). Subsequent analysis at 15 days post-treatment showed a 51% reduction in Tau protein levels in neurons treated with a high dose of CRISPRoff, indicating long-lasting repression of Tau protein after a single treatment. Collectively, these results underscore the ability of our RENDER platform to effectively deliver CRISPR-based epigenome editors into challenging cell types, such as neurons, for targeted epigenetic modulation in translational research and therapeutic applications.

Discussion

Here, we present RENDER as a robust platform for transient delivery of CRISPR-based epigenome editor ribonucleoproteins into human cells. RENDER can package diverse epigenome editors as cargo, including CRISPRi for short-term, reversible gene repression and CRISPRoff and DNMT3A-3L-dCas9 for durable gene silencing. RENDER takes advantage of the eVLP platform that has been established recently to deliver CRISPR nucleases, base editors and prime editors. We further optimized the RENDER platform specifically for CRISPRoff to increase protein and sgRNA cargo packaging, which improved its epigenetic silencing potency by 4.4-fold, yielding RENDER-CRISPRoff v3. A single dose of RENDER-CRISPRoff v3 induces efficient and durable epigenetic silencing of target genes for over a month and is functional across multiple cell types and different gene targets.

RNP delivery of CRISPR technologies offers several advantages over other delivery formulations due to its transient nature and minimized off-target editing. However, epigenome editors consist of chromatin modifying domains that are often difficult to purify at high concentrations *in vitro* for RNP delivery. For example, the widely used KRAB domain in CRISPRi and CRISPRoff is structurally disordered in the absence of its binding partner TRIM28[25,26]. In comparison, plasmid DNA transfections of CRISPRi/off into the same cells yield ~60% transfection efficiencies, necessitating the use of selection methods (e.g., cell sorting or antibiotic selection) to isolate a pure population of transfected cells[47]. Additionally, mRNA-based delivery requires electroporation, which impacts cell viability and is not amenable to every cell type, or lipid nanoparticle formulation that requires cell type-specific customization[22,24]. Our data highlight that eVLPs package functional epigenome editor RNPs, achieving titratable levels of transient (CRISPRi) and durable (CRISPRoff) silencing after a single dose treatment, with minimal effects on cell viability.

We showed that RENDER-based delivery of CRISPRoff results in robust silencing of endogenous genes in cultured human neurons, including notable repression of the Tau protein in neurons harboring a known pathogenic mutation. We envision further engineering efforts will lead to the next-generation RENDER platform for epigenome editors to increase efficacy, especially in cell types where we observed lower epigenetic silencing. For example, eliminating non-structural viral proteins, such as integrase and reverse transcriptase, from the gag-pol polyprotein may provide more capacity for cargo loading, as shown recently for HIV-based EDVs for Cas9 nuclease. By incorporating tissue-specific envelope proteins, the applications of RENDER can be further expanded to diverse tissues *in vivo*. Moreover, the high efficacy of CRISPRoff apoprotein delivery by RENDER paves a platform for CRISPR screens in sgRNA library-expressing cell lines that will advance functional genomics applications using epigenome editing perturbations.

Methods

Molecular cloning

All plasmids to express protein components were cloned using Gibson assembly. DNA was PCR amplified with KAPA HiFi HotStart ReadyMix PCR Kit (Roche). Plasmids were transformed into Top10 chemically competent *Escherichia coli* (Thermo Fisher Scientific) and were prepared using either QIAprep Spin Miniprep kits (Qiagen) or ZymoPURE II Plasmid Maxiprep Kit (Zymo Research). CRISPRoff (KOX1), CRISPRi (KOX1), DNMT3A-3L-dCas9, TET1-dCas9 and dCas9 sequences were PCR amplified from previous constructs[16] (Addgene #167981 and #167983) and cloned in to the eVLP backbone from pCMV-MMLVgag-3×NES-ABE8e (Addgene #181751) to replace the base editor ABE8e (Supplementary Table 1). The ZIM3 KRAB sequence was obtained from previous study[37], synthesized as a gBlock (IDT) and cloned into the CRISPRoff and CRISPRi construct to replace the KOX1 KRAB domain. Similar to CRISPRoff, all editors include a direct fusion of HA-tag, 2×SV40 NLS and BFP to the C-terminus of dCas9.

The transient sgRNA expression plasmid encodes for expression of a sgRNA from a modified U6 (mU6) promoter along with expression from an EF1α promoter of a puromycin resistance gene and mCherry separated by a T2A cleavage sequence. To generate a minimal plasmid backbone, the origin of replication and the ampicillin resistance gene from pUC19 and the terminator from the pCAG mammalian expression vector were PCR amplified with KAPA HiFi HotStart ReadyMix PCR Kit (Roche). The lentiviral pLG1 library vector (Addgene #217306) was digested with XbaI and EcoRI to obtain only the mU6-sgRNA and EF1α-puroR-T2A-mCherry sequence. The transient plasmid was constructed using Gibson assembly of these three fragments with NEBuilder® HiFi DNA Assembly (NEB).

To change the protospacers, the transient backbone was digested with BstXI and BlpI, which cut downstream of the mU6 promoter. The protospacer sequence (**Supplementary Table 2**) was then ordered as two complementary oligos (IDT) with compatible BstXI and BlpI overhangs and ligated into the cut vector. The protospacer sequences were chosen based on previous algorithms to predict active CRISPRi sgRNAs targeting gene promoters[1]. Additionally, a protospacer sequence targeting the *GAL4* gene in *Saccharomyces cerevisiae* was used as non-targeting sgRNA (**Supplementary Table 2**).

Tissue culture

All cell lines were obtained and authenticated by the UC Berkeley Cell Culture Facility. The CLTA-GFP and HIST2H2BE-GFP HEK293T cell lines originated from previous study[48]. Lenti-X, HEK293T, HeLa and HepG2 cells were cultured in DMEM (Gibco). Jurkat and K562 cells were cultured in RPMI-1640 (Gibco). h-TERT RPE-1 cells were cultured in DMEM/F-12, GlutaMAX. U87 and SH-SY5Y cells were cultured in DMEM, supplemented with 1% (v/v) MEM Non-Essential Amino Acids Solution (Gibco) and 1 mM sodium pyruvate (Gibco). All media was supplemented with 10% (v/v) FBS (VWR) and 100 U/ml streptomycin, 100 mg/ml penicillin (Gibco). Cell lines were cultured at 37 °C with 5% CO_2 in tissue culture incubators and routinely confirmed to be negative for mycoplasma.

408 **Generation of stable sgRNA expressing cell line**
409 To test the sgRNA-free CRISPRoff-eVLP, CLTA-GFP HEK293T reporter cells were transduced
410 with lentivirus to constitutively express a sgRNA targeting the *CLTA* promoter. Lentiviral particles
411 were produced by transient transfection of HEK293T cells. Cells were seeded at a density of 4.0
412 × 10^5 cells per well in a 6-well BioLite Microwell plate (Thermo Fisher Scientific) and co-
413 transfected the next day with standard packaging plasmids (0.1 µg gag-pol, REV, TAT, 0.2 µg
414 VSVG) and 1.5 µg lentiviral sgRNA expression vector (Addgene #217306) using Opti-MEM
415 (Gibco) and TransIT®-LT1 Transfection Reagent (Mirus Bio), following the manufacturer's
416 protocol. Media was changed 24 hours post-transfection with complete DMEM. Viral supernatants
417 were harvested 48-60 hours after transfection and filtered through a 0.45 µm PES syringe filter
418 (VWR). CLTA-GFP HEK293T cells were transduced with lentiviral particles and subsequently
419 sorted on mCherry expression to obtain a >99% sgRNA expressing cell line.
420
421 **Epigenome editor eVLP production and concentration**
422 Epigenome editor eVLPs were produced by transient transfection of Lenti-X 293T cells. Cells
423 were seeded at a density of 4 × 10^6 cells per 10-cm BioLite Cell Culture dish (Thermo Fisher
424 Scientific) and transfected the next day using Opti-MEM (Gibco) and TransIT®-LT1 Transfection
425 Reagent (Mirus Bio), following the manufacturer's protocol.
426
427 For the comparison of different epigenome editor eVLPs, cells were co-transfected with 0.5 µg
428 VSV-G (Addgene #8454), 3.0 µg gag-pol (Addgene #35614), 1.5 µg gag-editor and 5.0 µg mU6-
429 sgRNA plasmids. For stoichiometry optimization, the total amount of gag-CRISPRoff (ZIM3) and
430 gag-pol plasmid was fixed at 4.5 µg, while the ratio of gag-CRISPRoff (ZIM3) was varied from 10-
431 100%. For sgRNA optimization, a fixed stoichiometry of 90% gag-CRISPRoff (ZIM3) (4.05 µg)
432 and 10% gag-pol (0.45 µg) was used, while the amount of mU6-sgRNA plasmid was varied from
433 1.0 to 6.0 µg.
434
435 For packaging of the final optimized CRISPRoff-eVLP v3, cells were co-transfected with 0.5 µg
436 VSV-G, 0.45 µg gag-pol, 4.05 µg gag-CRISPRoff (ZIM3) and 6.0 µg mU6-sgRNA. For multiplexed
437 gene targeting, plasmids expressing different sgRNAs were pooled for co-transfection, keeping
438 the total amount of sgRNA plasmid at 6.0 µg. For protein-only CRISPRoff-eVLP v3, cells were
439 co-transfected with 1.0 µg VSV-G, 0.90 µg gag-pol and 8.1 µg gag-CRISPRoff (ZIM3).
440
441 Three days post transfection, editor-eVLP containing supernatant was collected, filtered through
442 a 0.45 µm PES syringe filter (VWR) and precipitated overnight using Lenti-X Concentrator (Takara
443 Bio) according to manufacturer's instructions. Editor-eVLPs were concentrated 100-fold by
444 resuspending in 100 µl Opti-MEM, frozen at a rate of -1 °C/min, and stored at -80 °C. Frozen
445 eVLPs were thawed on ice immediately before use.
446
447 **Editor-eVLP transduction and flow cytometry**
448 For adherent cells, 1.5 × 10^4 cells were plated for transduction in 200 µl media per well in a 96-
449 well plate (Corning). After 18-24 h, editor-eVLPs were directly added to the media. Suspension
450 cells were plated at 1.5 × 10^4 cells in 200 µl media per well and directly transduced with editor-
451 eVLPs by centrifugation at 1,500 *g* for 1.5 h at 32 °C.

For scaling-up eVLP transduction in Jurkat cells, non-treated 6-well or 96-well plates (Falcon) were coated with retronectin (Takara Bio) at a density of 8 µg/cm^2, following manufacturer's instructions. Jurkat cells were plated at 1.5 × 10^4 cells in 100 µl media per 96-well or 5.0 × 10^5 cells in 1.5 ml per 6-well and transduced with eVLPs by centrifugation at 1,500 × *g* for 1.5 h at 32 °C. 18-24 h post-transduction, 100 µl fresh media was added per 96-well or 1.5 ml per 6-well.

Treated cells were passaged every 2-3 days and durable target gene silencing was assessed by flow cytometric analysis. Protein expression was assessed by cell surface antibody staining of live cells. Cells were incubated with diluted antibody (**Supplementary Table 3**) for 30-60 min in the dark at room temperature, washed once with PBS and measured on the BD FACSymphony A1 Cell Analyzer (BD Biosciences). For the different GFP-tagged HEK293T reporter cell lines, protein expression was directly assessed by flow cytometry. Data analysis was performed using FlowJo (v10.10).

Isolation, activation and transduction of primary human T cells

Cryopreserved human peripheral blood mononuclear cells (STEMCELL Technologies) were thawed and T cells were isolated using EasySep Buffer and the EasySep Human T Cell Isolation Kit (STEMCELL Technologies) according to manufacturer's instructions. Naïve T cells were cultured in basal media comprised of X-VIVO 15 Serum-free Hematopoietic Cell Medium (Lonza) with 5% FBS (v/v) (VWR), 10 mM *N*-Acetyl-L-cysteine (Sigma-Aldrich) and 50 µM 2-mercaptoethanol (Gibco), or frozen for long-term storage in basal media, without FBS, supplemented with 10% DMSO.

Isolated or thawed naïve T cells were kept in basal media for 24 h and then activated by adding Dynabeads Human T-Activator CD3/CD28 (1:1 bead-to-cell ratio, Gibco), 300 U/ml recombinant human IL-2 (Peprotech), 5 ng/ml recombinant human IL-7 (Peprotech) and 5 ng/ml recombinant human IL-15 (R&D Systems). After two days of activation, magnetic beads were removed and T cells were cultured in basal media with 500 U/ml IL-2, 5 ng/ml IL-7 and 5 ng/ml IL-15.

For eVLP transduction, T cells were seeded at 5.0 × 10^4 cells in 100 µl media per well and 5 µl of CRISPRoff-eVLPs packaged with a pool of three sgRNAs for CD55 (a, b, c), or two sgRNA for CD81 (a, b) or a non-targeting (NT) sgRNA (Supplementary Table 2) were directly added to the media. For mRNA electroporation, 1.0 × 10^6 T cells were nucleofected with 1 µg of CRISPRoff mRNA (Aldeveron) and 2.5 µg of synthetic sgRNA in P3 Primary Cell 96-well Nucleofector kit as previously described[47]. Modified synthetic sgRNAs were ordered from Synthego with the same protospacer sequences for CD55 (a, b) or CD81 (a, b) and equally pooled for electroporation, or a non-targeting protospacer sequence (NT) (**Supplementary Table 2**). Treated T cells were cultured in basal media with 500 U/ml IL-2, 5 ng/ml IL-7 and 5 ng/ml IL-15 and passaged every 2-3 days. Target gene silencing was assessed by flow cytometric analysis, as described above, in combination with a viability dye (**Supplementary Table 3**).

493 **Differentiation and transduction of iPSC-derived neurons**
494 Neurons were derived from WTC-NGN2 iPSCs following a differentiation protocol as previously
495 described[45]. On the third day of differentiation (Day -7 relative to eVLP addition), neurons were
496 seeded onto PDL-coated culture plates (Corning #356414). In 24-well plate format, each well
497 contained ~100,000 cells and was treated with 5, 15, or 45 µl of eVLP-containing media. In larger
498 plate formats, these ratios were scaled up proportionally to the feeding volume.
499
500 Neurons were fixed with a Zinc fixation buffer (0.1 M Tris HCl pH 6.5, 0.5% $ZnCl_2$, 0.5% Zn Acetate
501 and 0.05% $CaCl_2$) at 4 °C overnight. For CD81 staining, the second day, after removing the
502 fixation solution, neurons were washed twice with PBS, then incubated with APC anti-human
503 CD81 (TAPA-1) antibody solution (1.25:100) for 1 h at RT. For Tau protein staining, the second
504 day, after removing the fixation solution, neurons were washed twice with PBS, then incubated
505 and permeabilized with permeabilization/blocking buffer (10% Goat Serum, 1% TBS, 3% BSA, 1%
506 glycine and 0.5% Tween-20) at RT for 30 min. After removing this solution and washing 2 times
507 with PBS, neurons were incubated with the following buffers at RT, with two PBS washes after
508 each incubation: primary antibody solution (1:1000, #sc-21796) for 1 h, secondary antibody
509 solution (1:500, #ab150117) for 1 h. After removing staining solution and washing 2 times with
510 PBS, neurons were then pelleted, resuspended in 300 µl of PBS per sample, and triturated gently
511 to singularize. These samples were passed through strainer-capped FACS tubes (eg Stellar Sci
512 #FSC-9005), and analyzed on an Attune NxT (Thermo Fisher Scientific). Results were interpreted
513 using FlowJo (v10.10).
514
515 **Western blot analysis**
516 Concentrated RENDER-CRISPRoff (v3) were denatured at 90 °C for 5 min in reducing Laemmli
517 SDS sample buffer (Thermo Fisher Scientific). Denatured proteins were separated on a NuPAGE
518 3-8% Tris-Acetate Gel (Thermo Fisher Scientific) in NuPAGE Tris-Acetate SDS Running Buffer
519 (Thermo Fisher Scientific) at 150 V for 1 h. Proteins were wet transferred into PVDF membrane
520 (Bio-Rad) in Tris-Glycine buffer (25 mM Tris-HCl, 250 mM glycine, 20% (v/v) ethanol) at 300 mA
521 for 2 h. The membrane was washed three times with TBS-T (20 mM Tris-HCl, 150 mM NaCl, 0.1%
522 Tween-20), blocked with 5% nonfat dry milk (Apex) in TBS-T at room temperature for 1 h and
523 incubated at 4 °C overnight with mouse-anti FLAG (1:400, Sigma-Aldrich, F3165) or mouse-anti
524 Cas9 (1:1,000, Active Motif, AB_2793684) in 1% milk TBS-T with gentle rocking. After three
525 washes with TBS-T, the membrane was incubated at room temperature for 1 h with goat anti-
526 mouse secondary antibody (1:10,000, LI-COR, IRDye 680RD) in TBS-T by rocking. The
527 membrane was washed three times with TBS-T and imaged on the Odyssey CLx (LI-COR).
528
529 **Whole genome DNA methylation sequencing and analysis**
530 We generated whole genome enzymatic methyl sequencing (WGEMS) libraries for 4 samples
531 corresponding to two technical replicates of wild-type (untreated) Jurkat cells and Jurkat cells
532 treated with RENDER-CRISPRoff targeting CD55. Genomic DNA was isolated using the
533 PureLink™ Genomic DNA Mini Kit (Invitrogen), 200 ng of DNA was diluted with TE buffer to 108
534 µl. Control DNA Unmethylated Lambda (NEB #E7122AVIAL) and Control DNA CpG methylated
535 pUC19 (NEB #E7123AVIAL) were diluted 1:50 with TE buffer and 1 µl was added to the genomic
536 DNA (final volume 110 µl). DNA samples were sheared using a Covaris S220 (peak incident

power: 175 W, duty factor: 10%, cycles per burst: 200, treatment time: 180 s). 50 µl of sheared DNA was used for enzymatic methyl conversion following the NEBNext® Enzymatic Methyl-seq Kit (NEB #E7120S/L) for standard libraries using the formamide denaturation protocol. 5 ng of deaminated DNA was PCR-amplified for 6 cycles, followed by PCR-clean up and eluted in TE buffer according to protocol. Amplified libraries were quantified on an Agilent 2100 TapeStation system (Agilent) and equally pooled to a final concentration of 2.475 ng/µl in 50 µl (approximately 10 nM at 375 bp). The prepared libraries were sequenced paired-end 150 bp reads on an Illumina NovaSeq X 1.5B 2 Lanes (1.5 billion clusters). We obtained between 338.2M to 439.6M paired-end reads per library across all 4 libraries.

Reads were trimmed using cutadapt (version 4.9)[49], filtering empty resulting reads (-m 1) and specifying both forward (-a AGATCGGAAGAGCACACGTCTGAACTCCAGTCA) and reverse (-A AGATCGGAAGAGCGTCGTGTAGGGAAAGAGTGT) adapters. The resulting reads were aligned using Bismark (version 0.24.2)[50] to the hg38 reference genome with methylated and unmethylated control DNA sequences provided by NEBNext (https://neb-em-seq-sra.s3.amazonaws.com/grch38_core%2Bbs_controls.fa). The Bismark tools bismark_methylation_extractor and bismark2bedGraph were then used to create a methylation report, the top and bottom strand reads were combined (on the basis of CpG symmetry), and loci that had less then 10 mapped reads across the 8 methylation reports (top and bottom strands, four samples) were filtered out (approximately 2% of loci). Differential methylation analysis was performed using bsseq (version 1.40.0)[51] and DSS (version 2.52.0)[52] in R (version 4.4.1) by calling DMLtest with 500 bp smoothing. Plots were generated using Python (version 3.12.6) with Matplotlib (version 3.9.2)[53], NumPy (version 2.1.1), and Polars (version 1.9.0).

Acknowledgements

We thank Kevin Wasko for technical assistance and members of the Nuñez lab for helpful discussions. This work was funded by research grants awarded to J.K.N.: NIH R35 MIRA (R35GM155044-01), CRISPR Cures for Cancer Initiative (Gladstone Institutes, UCB 20240097), Bakar Labs (51474), and an Innovation Award from the Laboratory for Genomics Research (UCB 059006-001). J.K.N. and S.E.C. are Investigators of the Chan Zuckerberg Biohub - San Francisco. S.B. is funded by internship grants from the Nijbakker-Morra Stichting and Peter Grootenhuis Life Sciences. G.N.R. is funded by the Gladstone-CIRM Postdoctoral Fellowship. Neuron work was enabled by the Gladstone Stem Cell and Flow Cytometry Cores. J.P.L. is funded by a Graduate Research Fellowship from the National Science Foundation. R.K.P. is funded by graduate fellowships from the University of California Cancer Research Coordinating Committee and the Shurl and Kay Curci Foundation. I.J.O. is funded by graduate fellowships from the University of California, Berkeley Mentored Research Award, a Gilliam Fellowship from the Howard Hughes Medical Institute, and a National Science Foundation Graduate Research Fellowship. C.D.N. is a SURF Rose Hills Fellow and an Amgen Scholar at University of California, San Francisco.

Contributions

D.X., S.B. and J.K.N. led the study, designed the experiments and wrote the manuscript with assistance from the co-authors. D.X. and S.B. performed the majority of the RENDER experiments. G.N.R. and P.H.D. designed and performed the neuron editing experiments with supervision from B.R.C. J.P.L. and P.J.C. performed the WGEM-seq experiments and J.P.L. designed and analyzed the computational analysis pipeline under the supervision of S.E.C. R.K.P. and C.D.N. performed the T cell experiments. J.I.B. performed the TET1-dCas9 reactivation experiments and assisted with testing RENDER in different cell types. A.E.C. constructed the sgRNA expression plasmid and performed the H2B silencing experiments. I.J.O. assisted with computational data analysis.

Competing interests

J.K.N. and D.X. have filed a patent application related to the materials presented in this report. J.K.N. is an inventor of patents related to the CRISPRoff/on technologies, filed by The Regents of the University of California. B.R.C. is a founder of Tenaya Therapeutics and holds equity in the company.

592 **References**

593 1. Villiger, L. *et al.* CRISPR technologies for genome, epigenome and transcriptome editing. *Nature*
594 *Reviews Molecular Cell Biology* **25**, 464–487 (2024).
595 2. Doudna, J. A. The promise and challenge of therapeutic genome editing. *Nature* **578**, 229–236
596 (2020).
597 3. Wang, D., Zhang, F. & Gao, G. CRISPR-Based Therapeutic Genome Editing: Strategies and In Vivo
598 Delivery by AAV Vectors. *Cell* **181**, 136–150 (2020).
599 4. Fiumara, M. *et al.* Genotoxic effects of base and prime editing in human hematopoietic stem cells.
600 *Nature Biotechnology* **42**, 877–891 (2024).
601 5. Adikusuma, F. *et al.* Large deletions induced by Cas9 cleavage. *Nature* **560**, E8–E9 (2018).
602 6. Kosicki, M., Tomberg, K. & Bradley, A. Repair of double-strand breaks induced by CRISPR–Cas9 leads
603 to large deletions and complex rearrangements. *Nature Biotechnology* **36**, 765–771 (2018).
604 7. Haapaniemi, E., Botla, S., Persson, J., Schmierer, B. & Taipale, J. CRISPR–Cas9 genome editing
605 induces a p53-mediated DNA damage response. *Nature Medicine* **24**, 927–930 (2018).
606 8. Cullot, G. *et al.* CRISPR-Cas9 genome editing induces megabase-scale chromosomal truncations.
607 *Nature Communications* **10**, 1136 (2019).
608 9. Enache, O. M. *et al.* Cas9 activates the p53 pathway and selects for p53-inactivating mutations.
609 *Nature Genetics* **52**, 662–668 (2020).
610 10. Zuccaro, M. V. *et al.* Allele-Specific Chromosome Removal after Cas9 Cleavage in Human Embryos.
611 *Cell* **183**, 1650-1664.e15 (2020).
612 11. Tsuchida, C. A. *et al.* Mitigation of chromosome loss in clinical CRISPR-Cas9-engineered T cells. *Cell*
613 **186**, 4567-4582.e20 (2023).
614 12. Huang, M. E. *et al.* C-to-G editing generates double-strand breaks causing deletion, transversion and
615 translocation. *Nature Cell Biology* **26**, 294–304 (2024).

616 13. Zhu, M. *et al.* Tracking-seq reveals the heterogeneity of off-target effects in CRISPR–Cas9-mediated
617 genome editing. *Nature Biotechnology* (2024) doi:10.1038/s41587-024-02307-y.
618 14. Leibowitz, M. L. *et al.* Chromothripsis as an on-target consequence of CRISPR–Cas9 genome editing.
619 *Nature Genetics* **53**, 895–905 (2021).
620 15. McCutcheon, S. R., Rohm, D., Iglesias, N. & Gersbach, C. A. Epigenome editing technologies for
621 discovery and medicine. *Nature Biotechnology* **42**, 1199–1217 (2024).
622 16. Nuñez, J. K. *et al.* Genome-wide programmable transcriptional memory by CRISPR-based epigenome
623 editing. *Cell* **184**, 2503-2519.e17 (2021).
624 17. Amabile, A. *et al.* Inheritable Silencing of Endogenous Genes by Hit-and-Run Targeted Epigenetic
625 Editing. *Cell* **167**, 219-232.e14 (2016).
626 18. Cappelluti, M. A. *et al.* Durable and efficient gene silencing in vivo by hit-and-run epigenome editing.
627 *Nature* **627**, 416–423 (2024).
628 19. Neumann, E. N. *et al.* Brainwide silencing of prion protein by AAV-mediated delivery of an
629 engineered compact epigenetic editor. (2024).
630 20. Wu, Z., Yang, H. & Colosi, P. Effect of Genome Size on AAV Vector Packaging. *Molecular Therapy* **18**,
631 80–86 (2010).
632 21. Strebinger, D. *et al.* Cell type-specific delivery by modular envelope design. *Nat Commun* **14**, 5141
633 (2023).
634 22. Raguram, A., Banskota, S. & Liu, D. R. Therapeutic in vivo delivery of gene editing agents. *Cell* **185**,
635 2806–2827 (2022).
636 23. van Haasteren, J., Li, J., Scheideler, O. J., Murthy, N. & Schaffer, D. V. The delivery challenge: fulfilling
637 the promise of therapeutic genome editing. *Nature Biotechnology* **38**, 845–855 (2020).
638 24. Madigan, V., Zhang, F. & Dahlman, J. E. Drug delivery systems for CRISPR-based genome editors. *Nat*
639 *Rev Drug Discov* (2023) doi:10.1038/s41573-023-00762-x.

640 25. Stoll, G. A., Pandiloski, N., Douse, C. H. & Modis, Y. Structure and functional mapping of the KRAB-
641 KAP1 repressor complex. *The EMBO Journal* **41**, e111179 (2022).
642 26. Peng, H. *et al.* The Structurally Disordered KRAB Repression Domain Is Incorporated into a Protease
643 Resistant Core upon Binding to KAP-1-RBCC Domain. *Journal of Molecular Biology* **370**, 269–289
644 (2007).
645 27. Hamilton, J. R. *et al.* In vivo human T cell engineering with enveloped delivery vehicles. *Nat*
646 *Biotechnol* (2024).
647 28. Mangeot, P. E. *et al.* Genome editing in primary cells and in vivo using viral-derived Nanoblades
648 loaded with Cas9-sgRNA ribonucleoproteins. *Nat Commun* **10**, 45 (2019).
649 29. Hamilton, J. R. *et al.* Targeted delivery of CRISPR-Cas9 and transgenes enables complex immune cell
650 engineering. *Cell Reports* **35**, 109207 (2021).
651 30. Banskota, S. *et al.* Engineered virus-like particles for efficient in vivo delivery of therapeutic proteins.
652 *Cell* **185**, 250-265.e16 (2022).
653 31. An, M. *et al.* Engineered virus-like particles for transient delivery of prime editor ribonucleoprotein
654 complexes in vivo. *Nat Biotechnol* (2024) doi:10.1038/s41587-023-02078-y.
655 32. Lyu, P. *et al.* Adenine Base Editor Ribonucleoproteins Delivered by Lentivirus-Like Particles Show
656 High On-Target Base Editing and Undetectable RNA Off-Target Activities. *The CRISPR Journal* **4**, 69–
657 81 (2021).
658 33. Lu, Z. *et al.* Lentiviral Capsid-Mediated Streptococcus pyogenes Cas9 Ribonucleoprotein Delivery for
659 Efficient and Safe Multiplex Genome Editing. *The CRISPR Journal* **4**, 914–928 (2021).
660 34. Lyu, P., Javidi-Parsijani, P., Atala, A. & Lu, B. Delivering Cas9/sgRNA ribonucleoprotein (RNP) by
661 lentiviral capsid-based bionanoparticles for efficient 'hit-and-run' genome editing. *Nucleic Acids*
662 *Research* **47**, e99–e99 (2019).

663 35. Chandler, R. J., Sands, M. S. & Venditti, C. P. Recombinant Adeno-Associated Viral Integration and
664 Genotoxicity: Insights from Animal Models. *Human Gene Therapy* **28**, 314–322 (2017).
665 36. Replogle, J. M. *et al.* Maximizing CRISPRi efficacy and accessibility with dual-sgRNA libraries and
666 optimal effectors. *eLife* **11**, e81856 (2022).
667 37. Alerasool, N., Segal, D., Lee, H. & Taipale, M. An efficient KRAB domain for CRISPRi applications in
668 human cells. *Nat Methods* **17**, 1093–1096 (2020).
669 38. Nuñez, J. K. *et al.* Genome-wide programmable transcriptional memory by CRISPR-based epigenome
670 editing. *Cell* **184**, 2503-2519.e17 (2021).
671 39. O'Geen, H. *et al.* Ezh2-dCas9 and KRAB-dCas9 enable engineering of epigenetic memory in a
672 context-dependent manner. *Epigenetics & Chromatin* **12**, 26 (2019).
673 40. Policarpi, C., Munafò, M., Tsagkris, S., Carlini, V. & Hackett, J. A. Systematic epigenome editing
674 captures the context-dependent instructive function of chromatin modifications. *Nature Genetics*
675 **56**, 1168–1180 (2024).
676 41. Tycko, J. *et al.* Development of compact transcriptional effectors using high-throughput
677 measurements in diverse contexts. *Nature Biotechnology* (2024) doi:10.1038/s41587-024-02442-6.
678 42. Foss, D. V. *et al.* Peptide-mediated delivery of CRISPR enzymes for the efficient editing of primary
679 human lymphocytes. *Nat. Biomed. Eng* **7**, 647–660 (2023).
680 43. Aijaz, A. *et al.* Biomanufacturing for clinically advanced cell therapies. *Nature Biomedical*
681 *Engineering* **2**, 362–376 (2018).
682 44. Zhang, Z. *et al.* Efficient engineering of human and mouse primary cells using peptide-assisted
683 genome editing. *Nat Biotechnol* (2023) doi:10.1038/s41587-023-01756-1.
684 45. Ramadoss, G. N. *et al.* Neuronal DNA repair reveals strategies to influence CRISPR editing outcomes.
685 *bioRxiv* 2024.06.25.600517 (2024) doi:10.1101/2024.06.25.600517.

686 46. Mummery, C. J. *et al.* Tau-targeting antisense oligonucleotide MAPTRx in mild Alzheimer's disease: a
687 phase 1b, randomized, placebo-controlled trial. *Nature Medicine* **29**, 1437–1447 (2023).
688 47. Pattali, R. K. *et al.* CRISPRoff epigenetic editing for programmable gene silencing in human cells
689 without DNA breaks. *bioRxiv* 2024.09.09.612111 (2024) doi:10.1101/2024.09.09.612111.
690 48. Leonetti, M. D., Sekine, S., Kamiyama, D., Weissman, J. S. & Huang, B. A scalable strategy for high-
691 throughput GFP tagging of endogenous human proteins. *Proceedings of the National Academy of*
692 *Sciences* **113**, E3501–E3508 (2016).
693 49. Martin, M. Cutadapt removes adapter sequences from high-throughput sequencing reads.
694 *EMBnet.journal; Vol 17, No 1: Next Generation Sequencing Data AnalysisDO - 10.14806/ej.17.1.200*
695 (2011).
696 50. Krueger, F. & Andrews, S. R. Bismark: a flexible aligner and methylation caller for Bisulfite-Seq
697 applications. *Bioinformatics* **27**, 1571–1572 (2011).
698 51. Hansen, K. D., Langmead, B. & Irizarry, R. A. BSmooth: from whole genome bisulfite sequencing
699 reads to differentially methylated regions. *Genome Biology* **13**, R83 (2012).
700 52. Feng, H., Conneely, K. N. & Wu, H. A Bayesian hierarchical model to detect differentially methylated
701 loci from single nucleotide resolution sequencing data. *Nucleic Acids Research* **42**, e69–e69 (2014).
702 53. J. D. Hunter. Matplotlib: A 2D Graphics Environment. *Computing in Science & Engineering* **9**, 90–95
703 (2007).
704
705

Fig. 1: Virus-like particle delivery of epigenome editor RNPs.
a, Schematic of a virus-like particle packaging epigenome editors.
b, Schematic overview of different CRISPR-based epigenome editors and their sizes. kb; kilobase pairs.
c, Western blot evaluating the packaging of CRISPRoff protein in eVLPs at 4, 2 and 1 µl of concentrated CRISPRoff-eVLP with anti-Flag antibody.
d, Schematic of engineered virus-like particle transduction and CLTA-GFP silencing in HEK293T reporter cells.
e, Quantification of CLTA-GFP silencing in HEK293T cells 3 days post-treatment with different epigenome editor eVLPs (16 µl).
f, Representative flow cytometry plots of CLTA-GFP expression in HEK293T cells at day 3 and 14 post-treatment with CRISPRi-eVLPs and CRISPRoff-eVLPs (16 µl).
g, Time course of CLTA-GFP silencing in HEK293T cells post-treatment with different epigenome editor eVLPs (16 µl).
h, Schematic of virus-like particle transduction and CLTA-GFP reactivation in HEK293T reporter cells.
i, Time course of CLTA-GFP reactivation in HEK293T cells post-treatment with TET1-dCas9-eVLPs (32 µl).
j, Representative flow cytometry plots of CLTA-GFP expression in HEK293T cells 15 days post-treatment with TET1-dCas9-eVLP (32 µl).
All plot values represent the mean of three biological replicates and error bars represent the standard deviation.

Fig. 2: Optimizing RENDER-CRISPRoff composition.
a, Time course of CLTA-GFP silencing in HEK293T cells post-treatment with different doses of RENDER-CRISPRoff (ZIM3) (v1).
b, Time course of CLTA-GFP silencing in HEK293T cells post-treatment with different doses of RENDER-CRISPRi (ZIM3).
c, Schematic of optimization of RENDER-CRISPRoff.
d, Quantification of CLTA-GFP silencing in HEK293T cells 5 days post-treatment with 4 µl RENDER-CRISPRoff with varying gag-CRISPRoff to gag-pol plasmid ratios. X-axis indicates % gag-CRISPRoff plasmid of total amount of gag-CRISPRoff and gag-pol plasmids. Dark gray indicates v1, blue indicates v2.
e, Quantification of CLTA-GFP silencing in HEK293T cells 5 days post-treatment with 4 µl RENDER-CRISPRoff with varying amounts of sgRNA expressing plasmid. Blue indicates v2, magenta indicates v3.
f, Dose-response curve of CLTA-GFP silencing in HEK293T cells 5 days post-treatment with RENDER-CRISPRoff v1, v2 and v3. Data were fit to four-parameter logistic curves using nonlinear regression.
g, Time course of CLTA-GFP silencing in HEK293T cells post-treatment with RENDER-CRISPRoff v3 (16 µl).
h, Representative histogram plots of CLTA-GFP expression in HEK293T cells at day 3, 7, 14 and 49 post-treatment with RENDER-CRISPRoff v3 (16 µl). UT; untreated.
i, Representative histogram plots of H2B-GFP expression in HEK293T cells at day 3, 7, 14 and 29 post-treatment with RENDER-CRISPRoff v3 (10 µl). UT; untreated.
All plot values represent the mean of three biological replicates and error bars represent the standard deviation.

754 **Fig. 3: Multiplexed epigenetic silencing across diverse human cell types with RENDER-**
755 **CRISPRoff.**
756 **a**, Quantification of CD55 and CD81 silencing in different cell lines 7 days post-treatment with
757 RENDER-CRISPRoff v3 (8 µl). Values represent the mean of three biological replicates and error
758 bars represent the standard deviation. n.e.; not expressed.
759 **b**, Manhattan plot displaying differentially methylated CpGs between Jurkat cells treated with
760 RENDER-CRISPRoff v3 targeting *CD55* and untreated cells (14 days post-treatment) analyzed
761 by WGEM-seq. Magenta dots represent CpGs that gained DNA methylation in RENDER-
762 CRISPRoff-treated cells and blue dots represent CpGs that gained DNA methylation in untreated
763 cells. The arrow denotes the genomic location of the *CD55* gene.
764 **c**, Zoomed-in Manhattan plot displaying differentially methylated CpGs across a ±2 kilobase pairs
765 window from the *CD55* transcription start site (TSS) between Jurkat cells treated with RENDER-
766 CRISPRoff v3 targeting *CD55* and untreated cells (14 days post-treatment) analyzed by WGEM-
767 seq. Magenta dots represent CpGs that gained DNA methylation in RENDER-CRISPRoff-treated
768 cells and blue dots represent CpGs that gained DNA methylation in untreated cells. Annotated
769 CpG island (CGI) is shown in green and *CD55* targeting sgRNA in red.
770 **d**, Plot displaying the % of WGEM-seq reads that are methylated at each CpG across a ±2
771 kilobase pairs window from the *CD55* transcription start site (TSS) between Jurkat cells treated
772 with RENDER-CRISPRoff v3 targeting *CD55* (magenta) or untreated cells (blue) at 14 days post-
773 treatment. Annotated CpG island (CGI) is shown in green and *CD55* targeting sgRNA in red.
774 **e**, Schematic of multiplexing sgRNAs into one RENDER virus-like particle.
775 **f**, Representative flow cytometry plots of CD55 and CD81 expression in Jurkat cells 7 days post-
776 treatment with multiplexed RENDER-CRISPRoff v3 targeting *CD55* and *CD81* (8 µl).
777 **g**, Representative flow cytometry plots of CD55 and CD81 expression in U-87 MG cells 7 days
778 post-treatment with multiplexed RENDER-CRISPRoff v3 targeting *CD55* and *CD81* (8 µl).
779 **h**, Quantification of CLTA-GFP silencing in HEK293T cells 3 days post-treatment of 1.0×10^6
780 cells with different doses of RENDER-CRISPRoff v3. Values represent the mean of two biological
781 replicates and error bars represent the standard deviation.
782 **i**, Quantification of CD55 and CD81 silencing in Jurkat cells 3 days post-treatment of 5.0×10^5
783 cells with different doses of RENDER-CRISPRoff v3. Values represent the mean of one biological
784 replicate.
785 **j**, Schematic of sgRNA-free delivery of CRISPRoff apoprotein by RENDER and CLTA-GFP
786 silencing in HEK293T reporter cells stably expressing a *CLTA* targeting sgRNA.
787 **k**, Dose-response curve of CLTA-GFP silencing in HEK293T cells expressing a *CLTA* targeting
788 sgRNA 3 days post-treatment with sgRNA-free RENDER-CRISPRoff. Values represent the mean
789 of three biological replicates and error bars represent the standard deviation. Data were fit to four-
790 parameter logistic curves using nonlinear regression.

Fig. 4: Epigenome editing in primary human T cells.

a, Schematic of RENDER-CRISPRoff treatment and electroporation of isolated primary human T cells.

b, Representative flow cytometry plot showing the viability of T cells 2 days post RENDER-CRISPRoff or CRISPRoff-mRNA nucleofection with a *CD55* targeting sgRNA.

c, Quantification of live T cells 2 days post RENDER-CRISPRoff or CRISPRoff-mRNA electroporation, with *CD55* targeting or non-targeting (NT) sgRNA.

d, Representative histogram plots of CD55 expression in T cells at 2 and 11 days post-treatment with RENDER-CRISPRoff (5 µl) targeting *CD55* (orange) or non-targeting (gray). Percentages denote % cells with *CD55* silenced.

e, Representative histogram plots of CD55 expression in T cells at 2 and 11 days post-electroporation with CRISPRoff-mRNA and *CD55* targeting (orange) or non-targeting (gray) sgRNA. Percentages denote % cells with CD55 silenced.

f, Representative histogram plot of CD81 expression on T cells 11 days post-treatment with RENDER-CRISPRoff (5 µl) targeting *CD81* (blue) or non-targeting (gray), or post-electroporation with CRISPRoff-mRNA and *CD81* targeting (blue) or non-targeting (gray) sgRNA. Percentages denote % cells with CD81 silenced.

Fig. 5: Epigenome editing iPSC-derived neurons with RENDER.

a, Experimental workflow of gene knockdown by RENDER-CRISPRoff v3 in iPSC-derived neurons.

b, Representative histogram plots of CD81 expression in iPSC-derived neurons (wild-type) at day 7 and 14 post-treatment with different doses of RENDER-CRISPRoff v3 targeting *CD81* or non-targeting (NT).

c, Quantification of CD81 expression in iPSC-derived neurons (wild-type, WT) at day 7 and 14 post-treatment with different doses of RENDER-CRISPRoff v3 targeting *CD81*. CD81 expression is measured by antibody staining and flow cytometry and normalized to non-targeting (NT) control.

d, Representative histogram plots of Tau expression in iPSC-derived neurons (V337M mutant) at day 8 and 15 post-treatment with different doses of RENDER-CRISPRoff v3 targeting *MAPT* or non-targeting (NT).

e, Quantification of Tau expression in iPSC-derived neurons (V337M mutant) at day 8 and 15 post-treatment with different doses of RENDER-CRISPRoff v3 targeting *MAPT*. Tau expression is measured by antibody staining and flow cytometry and normalized to non-targeting (NT) control.

Extended Data Fig. 1. RENDER delivery of different epigenome editors into HEK293T.
Extended Data Fig. 1a, Representative flow cytometry plots showing the gating strategy for quantifying target gene silencing in CLTA-GFP HEK293T reporter cells.
Extended Data Fig. 1b, Dose-response curve of CLTA-GFP silencing in HEK293T cells 5 days post-treatment with CRISPRi-eVLP with the ZIM3 or KOX1 KRAB domain. Data were fit to four-parameter logistic curves using nonlinear regression.
Extended Data Fig. 1c, Dose-response curve of CLTA-GFP silencing in HEK293T cells 5 days post-treatment with CRISPRoff-eVLP with the ZIM3 or KOX1 KRAB domain. Data were fit to four-parameter logistic curves using nonlinear regression.
Extended Data Fig. 1d, Representative histograms of CLTA-GFP expression in HEK293T cells at day 3 and 14 post-treatment, each treated with the indicated epigenome editor eVLP.

Extended Data Fig. 2. Dose titration of different epigenome editors.
Extended Fig. 2a, Time course of CLTA-GFP silencing in HEK293T cells post-treatment with different doses of RENDER-dCas9.
Extended Fig. 2a, Time course of CLTA-GFP silencing in HEK293T cells post-treatment with different doses of RENDER-CRISPRi (KOX1).
Extended Fig. 2a, Time course of CLTA-GFP silencing in HEK293T cells post-treatment with different doses of RENDER-DNMT3A-3L-dCas9.
Extended Fig. 2a, Time course of CLTA-GFP silencing in HEK293T cells post-treatment with different doses of RENDER-CRISPRoff (KOX1).

Extended Data Fig. 3. Optimization of RENDER-CRISPRoff composition and transduction.
Extended Data Fig. 3a, Dose-response curve of CLTA-GFP silencing in HEK293T cells 5 days post-treatment with RENDER-CRISPRoff with varying gag-CRISPRoff to gag-pol plasmid ratios. Label indicates % gag-CRISPRoff plasmid of total amount of gag-CRISPRoff and gag-pol plasmids. Blue indicates v2. Data were fit to four-parameter logistic curves using nonlinear regression.
Extended Data Fig. 3b, Dose-response curve of CLTA-GFP silencing in HEK293T cells 5 days post-treatment with RENDER-CRISPRoff with varying amounts of sgRNA expressing plasmid. Blue indicates v2, magenta indicates v3. Data were fit to four-parameter logistic curves using nonlinear regression.
Extended Data Fig. 3c, Quantification of CD29, CD55, CD81 and CD151 silencing in Jurkat cells 14 days post treatment with RENDER-CRISPRoff v3 packaged with individual sgRNAs (a-c) or a pool of three sgRNAs (a, b, c).
Extended Data Fig. 3d, Quantification of CD55 silencing in Jurkat cells 3 days post treatment with different doses of RENDER-CRISPRoff v3, comparing retronectin-coated and uncoated plates for transduction.
Extended Data Fig. 3e, Quantification of CD55 silencing in Jurkat cells 14 days post treatment with different doses of RENDER-CRISPRoff v3, comparing retronectin-coated and uncoated plates for transduction.

870 **Extended Data Fig. 4. Analysis of increased DNA methylation after RENDER-CRISPRoff**
871 **treatment.**
872 **Extended Data Fig 4a-j**, Top ten most significant regions that are more methylated in RENDER-
873 CRISPRoff treated versus untreated Jurkat cells, as analyzed by whole-genome EM-seq.
874 Magenta dots represent CpGs that gained DNA methylation in RENDER-CRISPRoff-treated cells
875 and blue dots represent CpGs that gained DNA methylation in untreated cells. Black bars denote
876 genes.
877
878
879 **Extended Data Fig. 5. Analysis of decreased DNA methylation after RENDER-CRISPRoff**
880 **treatment.**
881 **Extended Data Fig 5a-j**, Top ten most significant regions that are more methylated in untreated
882 versus RENDER-CRISPRoff treated Jurkat cells, as analyzed by whole-genome EM-seq.
883 Magenta dots represent CpGs that gained DNA methylation in RENDER-CRISPRoff-treated cells
884 and blue dots represent CpGs that gained DNA methylation in untreated cells. Black bars denote
885 genes.

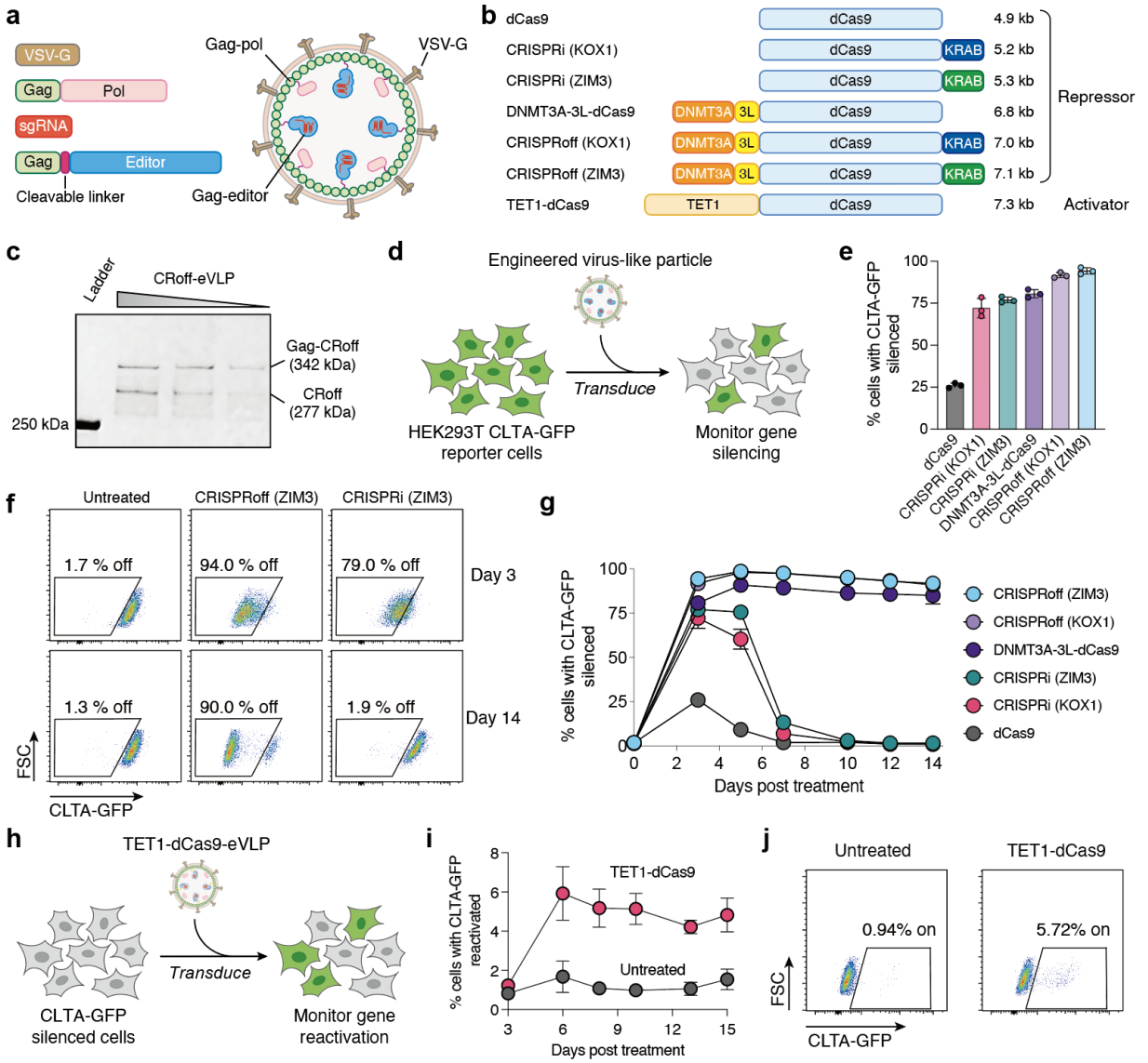

Fig. 1: Virus-like particle delivery of epigenome editor RNPs.

a, Schematic of a virus-like particle packaging epigenome editors.

b, Schematic overview of different CRISPR-based epigenome editors and their sizes. kb; kilobase pairs.

c, Western blot evaluating the packaging of CRISPRoff protein in eVLPs at 4, 2 and 1 µl of concentrated CRISPRoff-eVLP with anti-Flag antibody.

d, Schematic of engineered virus-like particle transduction and CLTA-GFP silencing in HEK293T reporter cells.

e, Quantification of CLTA-GFP silencing in HEK293T cells 3 days post-treatment with different epigenome editor eVLPs (16 µl).

f, Representative flow cytometry plots of CLTA-GFP expression in HEK293T cells at day 3 and 14 post-treatment with CRISPRi-eVLPs and CRISPRoff-eVLPs (16 µl).

g, Time course of CLTA-GFP silencing in HEK293T cells post-treatment with different epigenome editor eVLPs (16 µl).

h, Schematic of virus-like particle transduction and CLTA-GFP reactivation in HEK293T reporter cells.

i, Time course of CLTA-GFP reactivation in HEK293T cells post-treatment with TET1-dCas9-eVLPs (32 µl).

j, Representative flow cytometry plots of CLTA-GFP expression in HEK293T cells 15 days post-treatment with TET1-dCas9-eVLP (32 µl).

All plot values represent the mean of three biological replicates and error bars represent the standard deviation.

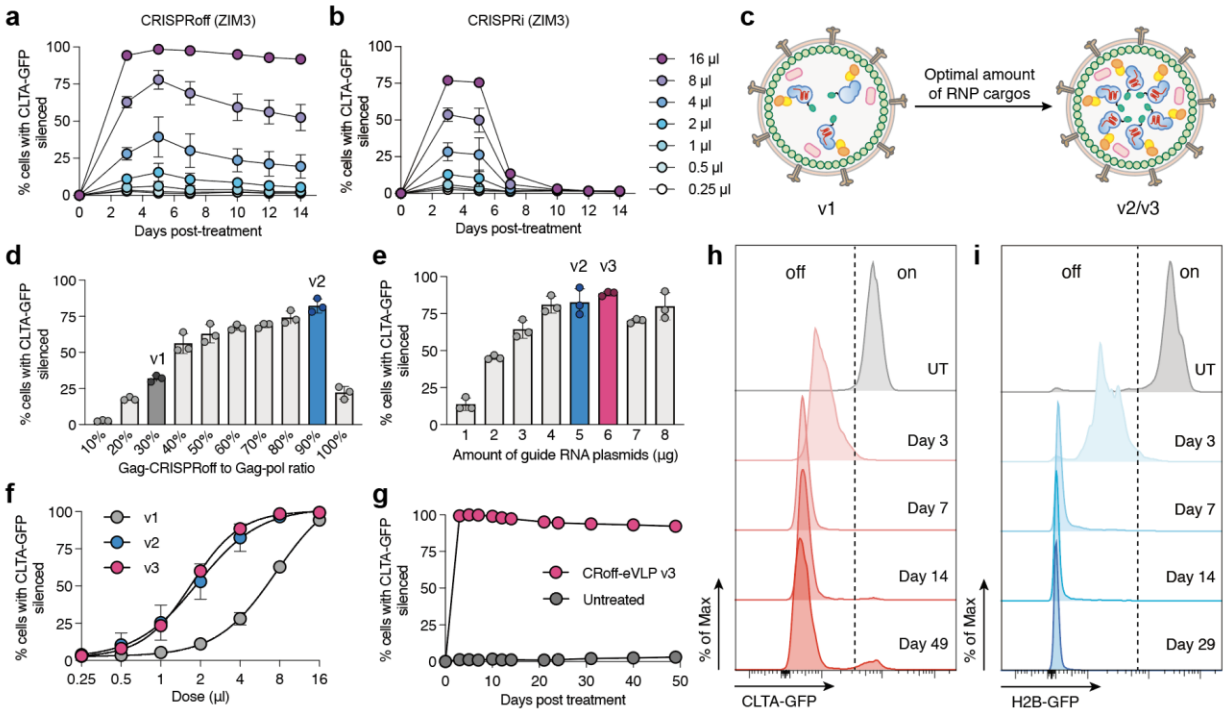

Fig. 2: Optimizing RENDER-CRISPRoff composition.

a, Time course of CLTA-GFP silencing in HEK293T cells post-treatment with different doses of RENDER-CRISPRoff (ZIM3) (v1).

b, Time course of CLTA-GFP silencing in HEK293T cells post-treatment with different doses of RENDER-CRISPRi (ZIM3).

c, Schematic of optimization of RENDER-CRISPRoff.

d, Quantification of CLTA-GFP silencing in HEK293T cells 5 days post-treatment with 4 µl RENDER-CRISPRoff with varying gag-CRISPRoff to gag-pol plasmid ratios. X-axis indicates % gag-CRISPRoff plasmid of total amount of gag-CRISPRoff and gag-pol plasmids. Dark gray indicates v1, blue indicates v2.

e, Quantification of CLTA-GFP silencing in HEK293T cells 5 days post-treatment with 4 µl RENDER-CRISPRoff with varying amounts of sgRNA expressing plasmid. Blue indicates v2, magenta indicates v3.

f, Dose-response curve of CLTA-GFP silencing in HEK293T cells 5 days post-treatment with RENDER-CRISPRoff v1, v2 and v3. Data were fit to four-parameter logistic curves using nonlinear regression.

g, Time course of CLTA-GFP silencing in HEK293T cells post-treatment with RENDER-CRISPRoff v3 (16 µl).

h, Representative histogram plots of CLTA-GFP expression in HEK293T cells at day 3, 7, 14 and 49 post-treatment with RENDER-CRISPRoff v3 (16 µl). UT; untreated.

i, Representative histogram plots of H2B-GFP expression in HEK293T cells at day 3, 7, 14 and 29 post-treatment with RENDER-CRISPRoff v3 (10 µl). UT; untreated.

All plot values represent the mean of three biological replicates and error bars represent the standard deviation.

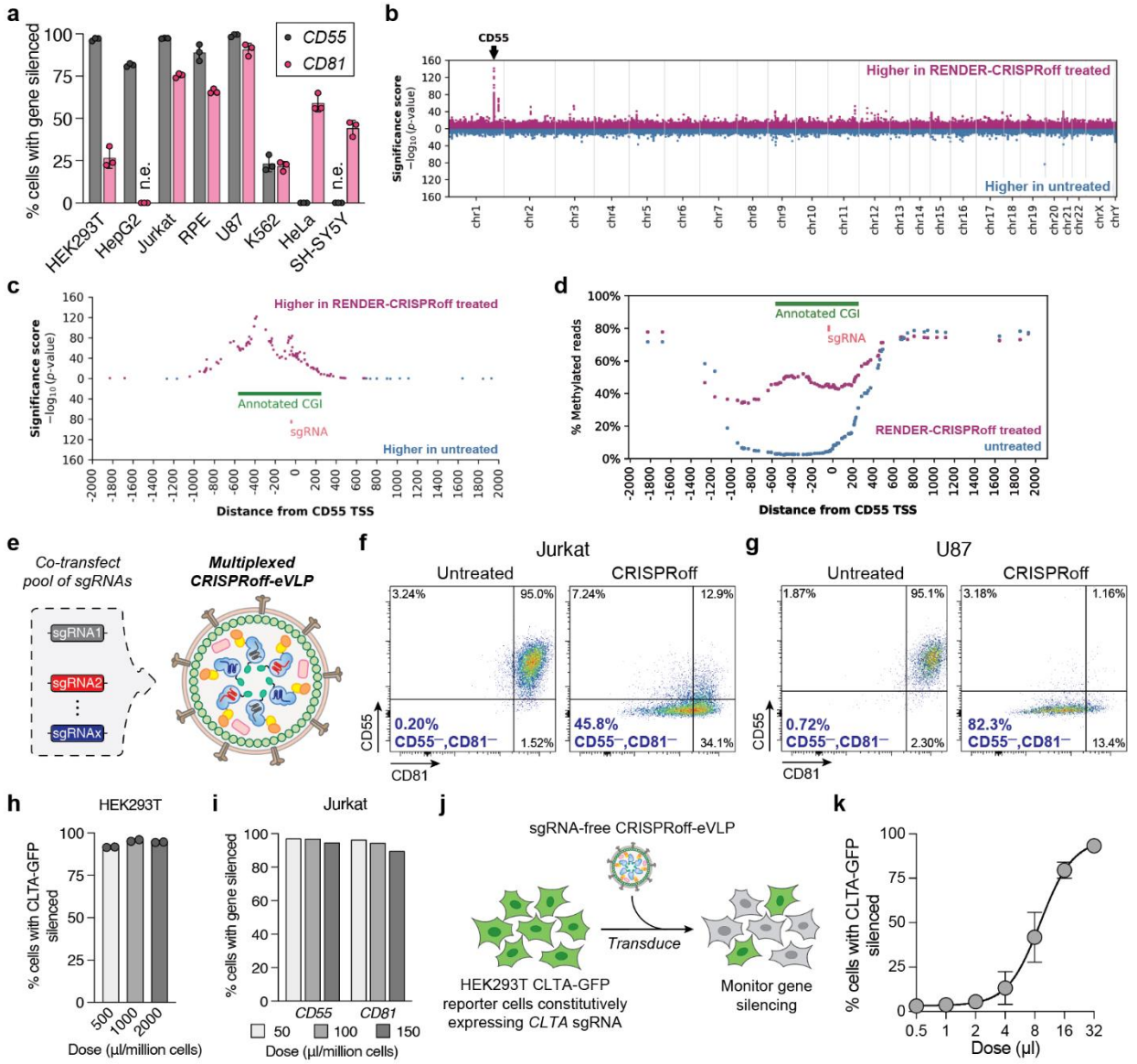

Fig. 3: Multiplexed epigenetic silencing across diverse human cell types with RENDER-CRISPRoff.

a, Quantification of CD55 and CD81 silencing in different cell lines 7 days post-treatment with RENDER-CRISPRoff v3 (8 µl). Values represent the mean of three biological replicates and error bars represent the standard deviation. n.e.; not expressed.

b, Manhattan plot displaying differentially methylated CpGs between Jurkat cells treated with RENDER-CRISPRoff v3 targeting *CD55* and untreated cells (14 days post-treatment) analyzed by WGEM-seq. Magenta dots represent CpGs that gained DNA methylation in RENDER-CRISPRoff-treated cells and blue dots represent CpGs that gained DNA methylation in untreated cells. The arrow denotes the genomic location of the *CD55* gene.

c, Zoomed-in Manhattan plot displaying differentially methylated CpGs across a ±2 kilobase pairs window from the *CD55* transcription start site (TSS) between Jurkat cells treated with RENDER-CRISPRoff v3 targeting *CD55* and untreated cells (14 days post-treatment) analyzed by WGEM-seq. Magenta dots represent CpGs that gained DNA methylation in RENDER-CRISPRoff-treated cells and blue dots represent CpGs that gained DNA methylation in untreated cells. Annotated CpG island (CGI) is shown in green and *CD55* targeting sgRNA in red.

d, Plot displaying the % of WGEM-seq reads that are methylated at each CpG across a ±2 kilobase pairs window from the *CD55* transcription start site (TSS) between Jurkat cells treated with RENDER-CRISPRoff v3 targeting *CD55* (magenta) or untreated cells (blue) at 14 days post-treatment. Annotated CpG island (CGI) is shown in green and *CD55* targeting sgRNA in red.

e, Schematic of multiplexing sgRNAs into one RENDER virus-like particle.
f, Representative flow cytometry plots of CD55 and CD81 expression in Jurkat cells 7 days post-treatment with multiplexed RENDER-CRISPRoff v3 targeting *CD55* and *CD81* (8 µl).
g, Representative flow cytometry plots of CD55 and CD81 expression in U-87 MG cells 7 days post-treatment with multiplexed RENDER-CRISPRoff v3 targeting *CD55* and *CD81* (8 µl).
h, Quantification of CLTA-GFP silencing in HEK293T cells 3 days post-treatment of 1.0×10^6 cells with different doses of RENDER-CRISPRoff v3. Values represent the mean of two biological replicates and error bars represent the standard deviation.
i, Quantification of CD55 and CD81 silencing in Jurkat cells 3 days post-treatment of 5.0×10^5 cells with different doses of RENDER-CRISPRoff v3. Values represent the mean of one biological replicate.
j, Schematic of sgRNA-free delivery of CRISPRoff apoprotein by RENDER and CLTA-GFP silencing in HEK293T reporter cells stably expressing a *CLTA* targeting sgRNA.
k, Dose-response curve of CLTA-GFP silencing in HEK293T cells expressing a *CLTA* targeting sgRNA 3 days post-treatment with sgRNA-free RENDER-CRISPRoff. Values represent the mean of three biological replicates and error bars represent the standard deviation. Data were fit to four-parameter logistic curves using nonlinear regression.

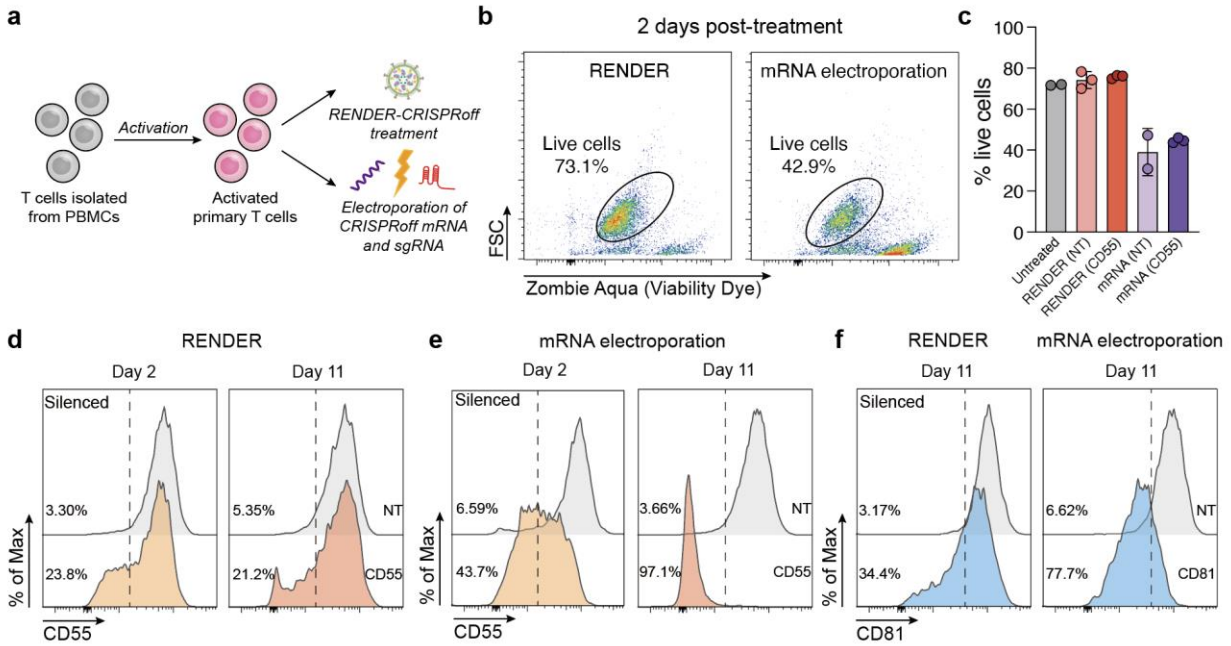

Fig. 4: Epigenome editing in primary human T cells.

a, Schematic of RENDER-CRISPRoff treatment and electroporation of isolated primary human T cells.

b, Representative flow cytometry plot showing the viability of T cells 2 days post RENDER-CRISPRoff or CRISPRoff-mRNA nucleofection with a *CD55* targeting sgRNA.

c, Quantification of live T cells 2 days post RENDER-CRISPRoff or CRISPRoff-mRNA electroporation, with *CD55* targeting or non-targeting (NT) sgRNA.

d, Representative histogram plots of CD55 expression in T cells at 2 and 11 days post-treatment with RENDER-CRISPRoff (5 µl) targeting *CD55* (orange) or non-targeting (gray). Percentages denote % cells with *CD55* silenced.

e, Representative histogram plots of CD55 expression in T cells at 2 and 11 days post-electroporation with CRISPRoff-mRNA and *CD55* targeting (orange) or non-targeting (gray) sgRNA. Percentages denote % cells with CD55 silenced.

f, Representative histogram plot of CD81 expression on T cells 11 days post-treatment with RENDER-CRISPRoff (5 µl) targeting *CD81* (blue) or non-targeting (gray), or post-electroporation with CRISPRoff0mRNA and *CD81* targeting (blue) or non-targeting (gray) sgRNA. Percentages denote % cells with CD81 silenced.

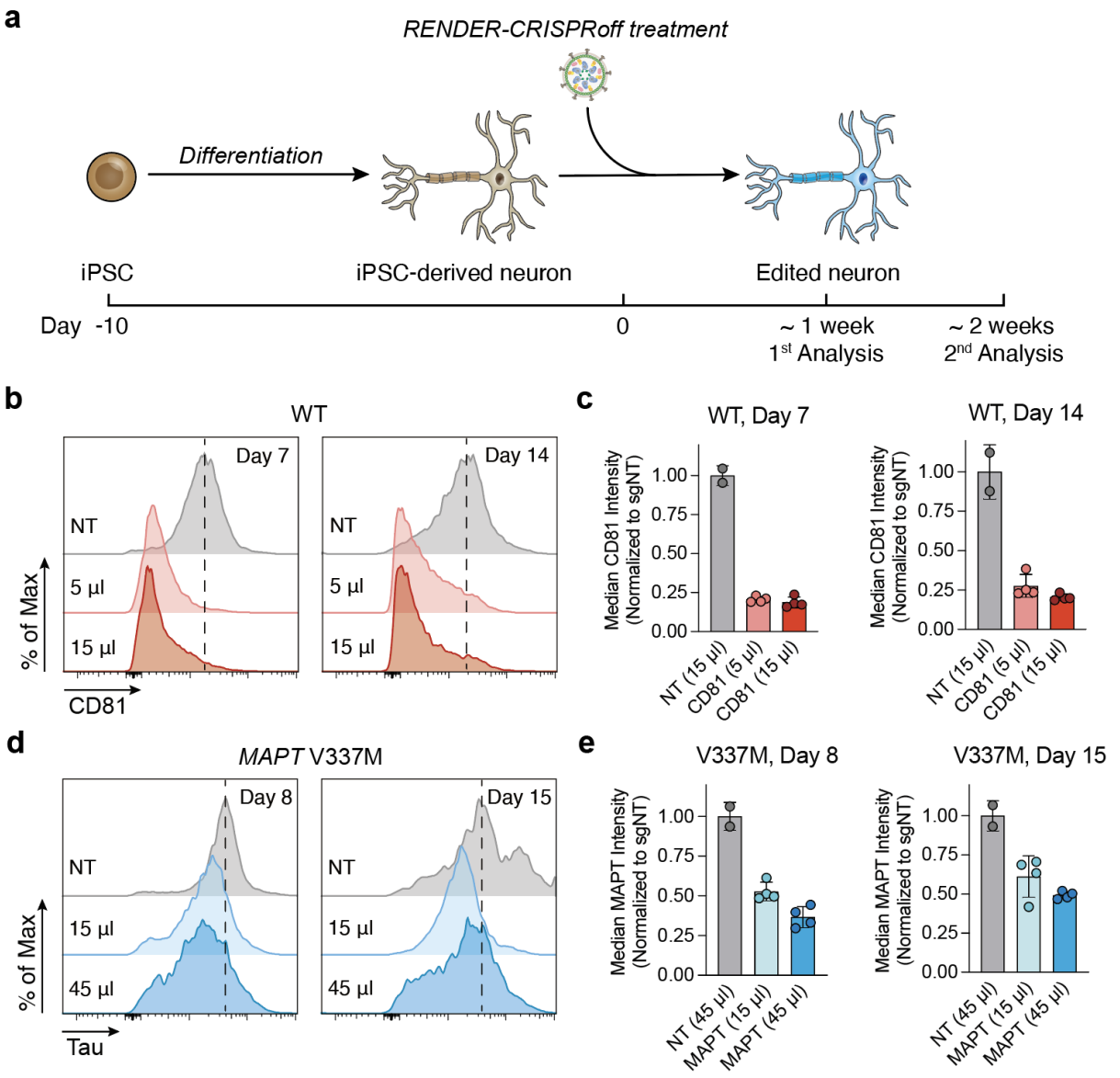

Fig. 5: Epigenome editing iPSC-derived neurons with RENDER.

a, Experimental workflow of gene knockdown by RENDER-CRISPRoff v3 in iPSC-derived neurons.

b, Representative histogram plots of CD81 expression in iPSC-derived neurons (wild-type) at day 7 and 14 post-treatment with different doses of RENDER-CRISPRoff v3 targeting *CD81* or non-targeting (NT).

c, Quantification of CD81 expression in iPSC-derived neurons (wild-type, WT) at day 7 and 14 post-treatment with different doses of RENDER-CRISPRoff v3 targeting *CD81*. CD81 expression is measured by antibody staining and flow cytometry and normalized to non-targeting (NT) control.

d, Representative histogram plots of Tau expression in iPSC-derived neurons (V337M mutant) at day 8 and 15 post-treatment with different doses of RENDER-CRISPRoff v3 targeting *MAPT* or non-targeting (NT).

e, Quantification of Tau expression in iPSC-derived neurons (V337M mutant) at day 8 and 15 post-treatment with different doses of RENDER-CRISPRoff v3 targeting *MAPT*. Tau expression is measured by antibody staining and flow cytometry and normalized to non-targeting (NT) control.

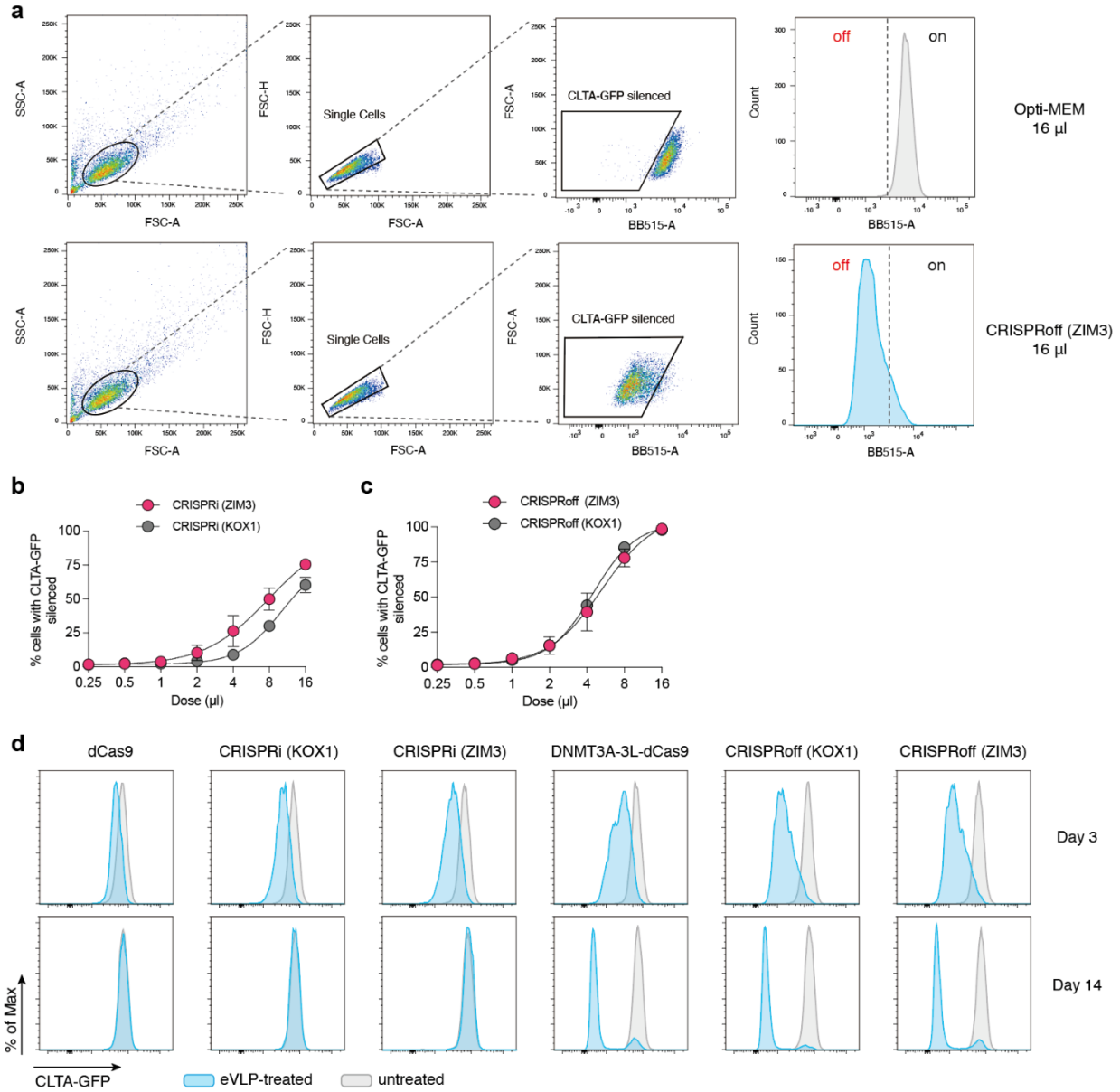

Extended Data Fig. 1. RENDER delivery of different epigenome editors into HEK293T.

Extended Data Fig. 1a, Representative flow cytometry plots showing the gating strategy for quantifying target gene silencing in CLTA-GFP HEK293T reporter cells.

Extended Data Fig. 1b, Dose-response curve of CLTA-GFP silencing in HEK293T cells 5 days post-treatment with CRISPRi-eVLP with the ZIM3 or KOX1 KRAB domain. Data were fit to four-parameter logistic curves using nonlinear regression.

Extended Data Fig. 1c, Dose-response curve of CLTA-GFP silencing in HEK293T cells 5 days post-treatment with CRISPRoff-eVLP with the ZIM3 or KOX1 KRAB domain. Data were fit to four-parameter logistic curves using nonlinear regression.

Extended Data Fig. 1d, Representative histograms of CLTA-GFP expression in HEK293T cells at day 3 and 14 post-treatment, each treated with the indicated epigenome editor eVLP.

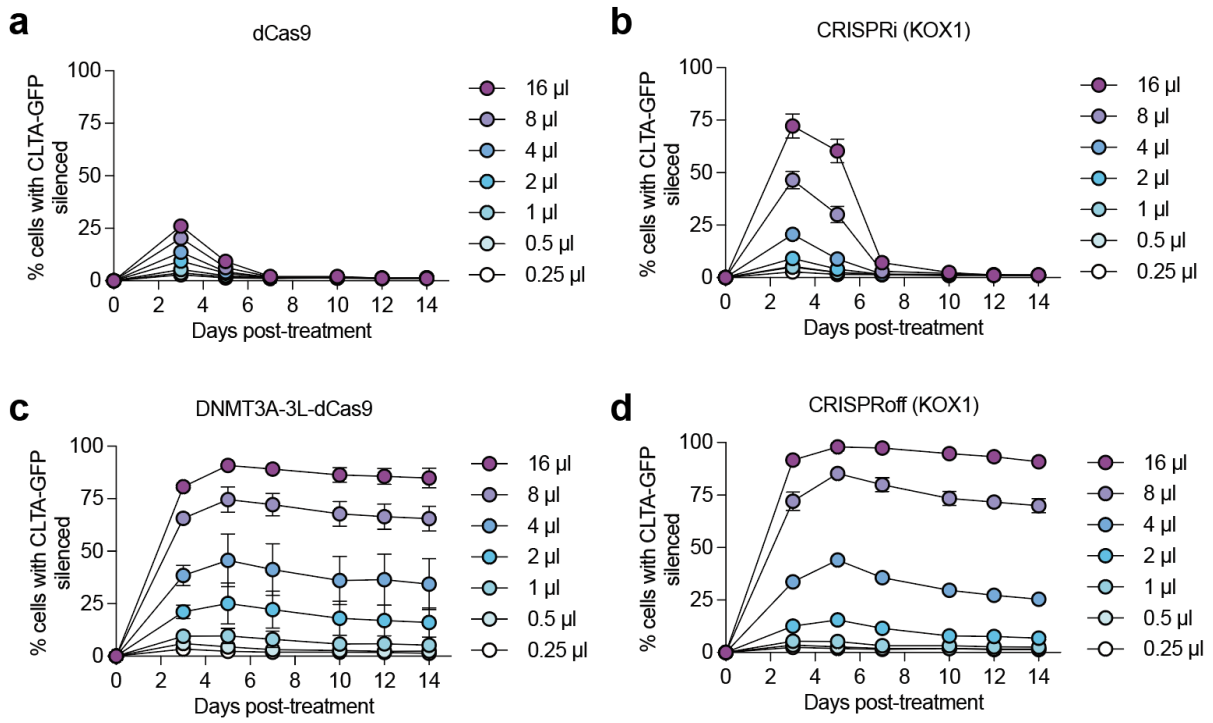

Extended Data Fig. 2. Dose titration of different epigenome editors.

Extended Fig. 2a, Time course of CLTA-GFP silencing in HEK293T cells post-treatment with different doses of RENDER-dCas9.

Extended Fig. 2a, Time course of CLTA-GFP silencing in HEK293T cells post-treatment with different doses of RENDER-CRISPRi (KOX1).

Extended Fig. 2a, Time course of CLTA-GFP silencing in HEK293T cells post-treatment with different doses of RENDER-DNMT3A-3L-dCas9.

Extended Fig. 2a, Time course of CLTA-GFP silencing in HEK293T cells post-treatment with different doses of RENDER-CRISPRoff (KOX1).

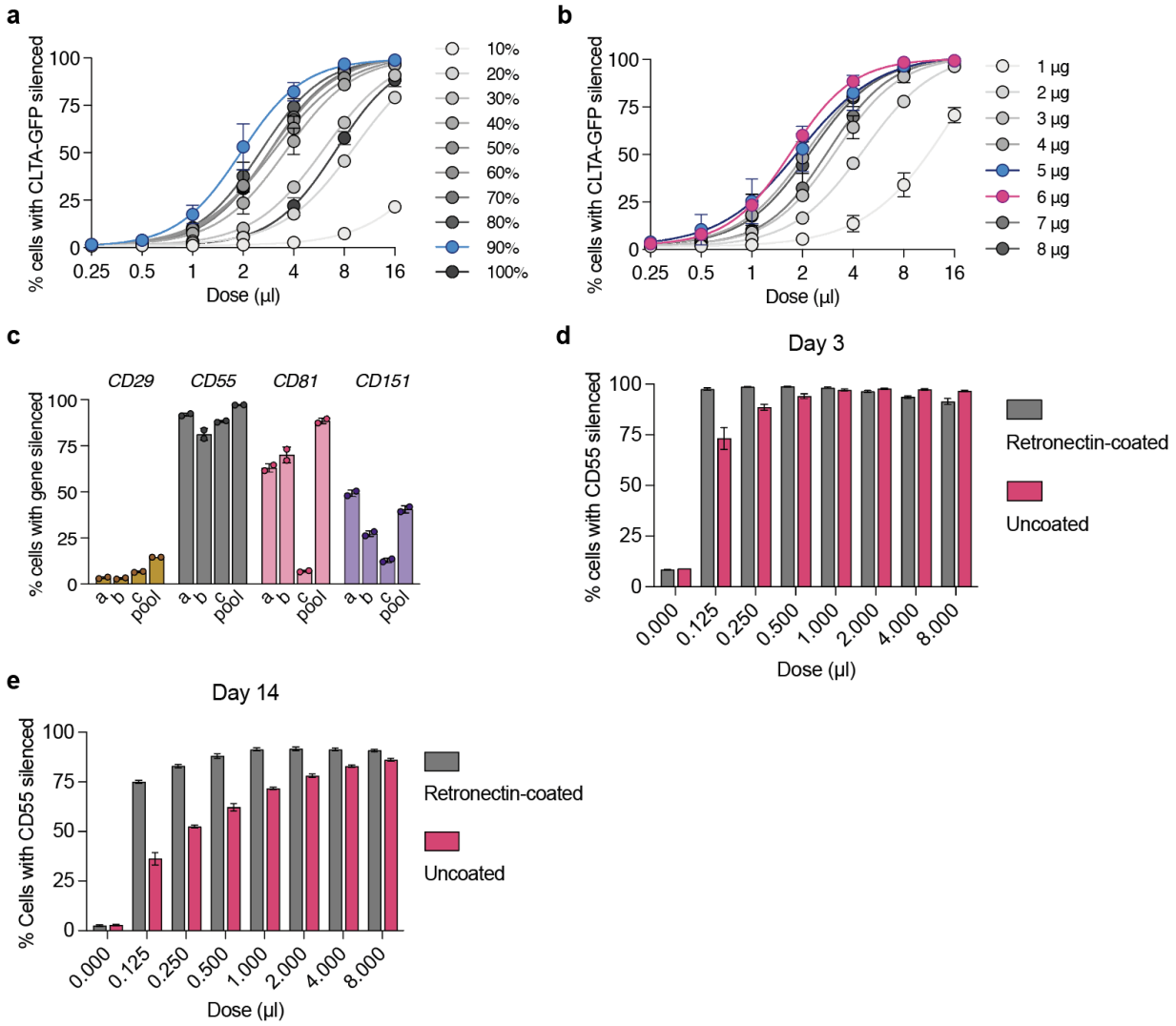

Extended Data Fig. 3. Optimization of RENDER-CRISPRoff composition and transduction.
Extended Data Fig. 3a, Dose-response curve of CLTA-GFP silencing in HEK293T cells 5 days post-treatment with RENDER-CRISPRoff with varying gag-CRISPRoff to gag-pol plasmid ratios. Label indicates % gag-CRISPRoff plasmid of total amount of gag-CRISPRoff and gag-pol plasmids. Blue indicates v2. Data were fit to four-parameter logistic curves using nonlinear regression.
Extended Data Fig. 3b, Dose-response curve of CLTA-GFP silencing in HEK293T cells 5 days post-treatment with RENDER-CRISPRoff with varying amounts of sgRNA expressing plasmid. Blue indicates v2, magenta indicates v3. Data were fit to four-parameter logistic curves using nonlinear regression.
Extended Data Fig. 3c, Quantification of CD29, CD55, CD81 and CD151 silencing in Jurkat cells 14 days post treatment with RENDER-CRISPRoff v3 packaged with individual sgRNAs (a-c) or a pool of three sgRNAs (a, b, c).
Extended Data Fig. 3d, Quantification of CD55 silencing in Jurkat cells 3 days post treatment with different doses of RENDER-CRISPRoff v3, comparing retronectin-coated and uncoated plates for transduction.
Extended Data Fig. 3e, Quantification of CD55 silencing in Jurkat cells 14 days post treatment with different doses of RENDER-CRISPRoff v3, comparing retronectin-coated and uncoated plates for transduction.

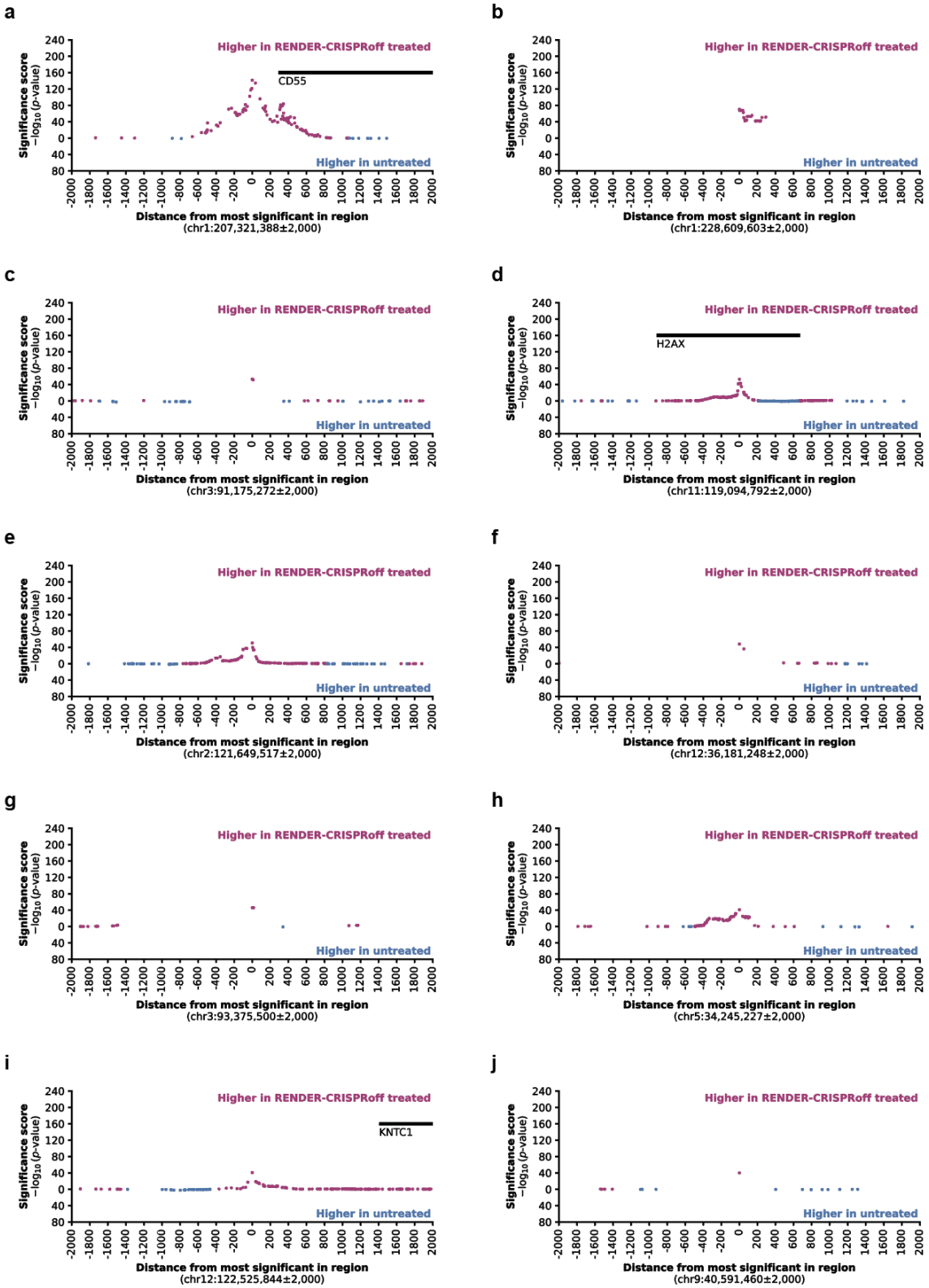

Extended Data Fig. 4: Analysis of increased DNA methylation after RENDER-CRISPRoff treatment.

Extended Data Fig. 4a-j, Top ten most significant regions that are more methylated in RENDER-CRISPRoff treated versus untreated Jurkat cells, as analyzed by whole-genome EM-seq. Magenta dots represent CpGs that gained DNA methylation in RENDER-CRISPRoff-treated cells and blue dots represent CpGs that gained DNA methylation in untreated cells. Black bars denote genes.

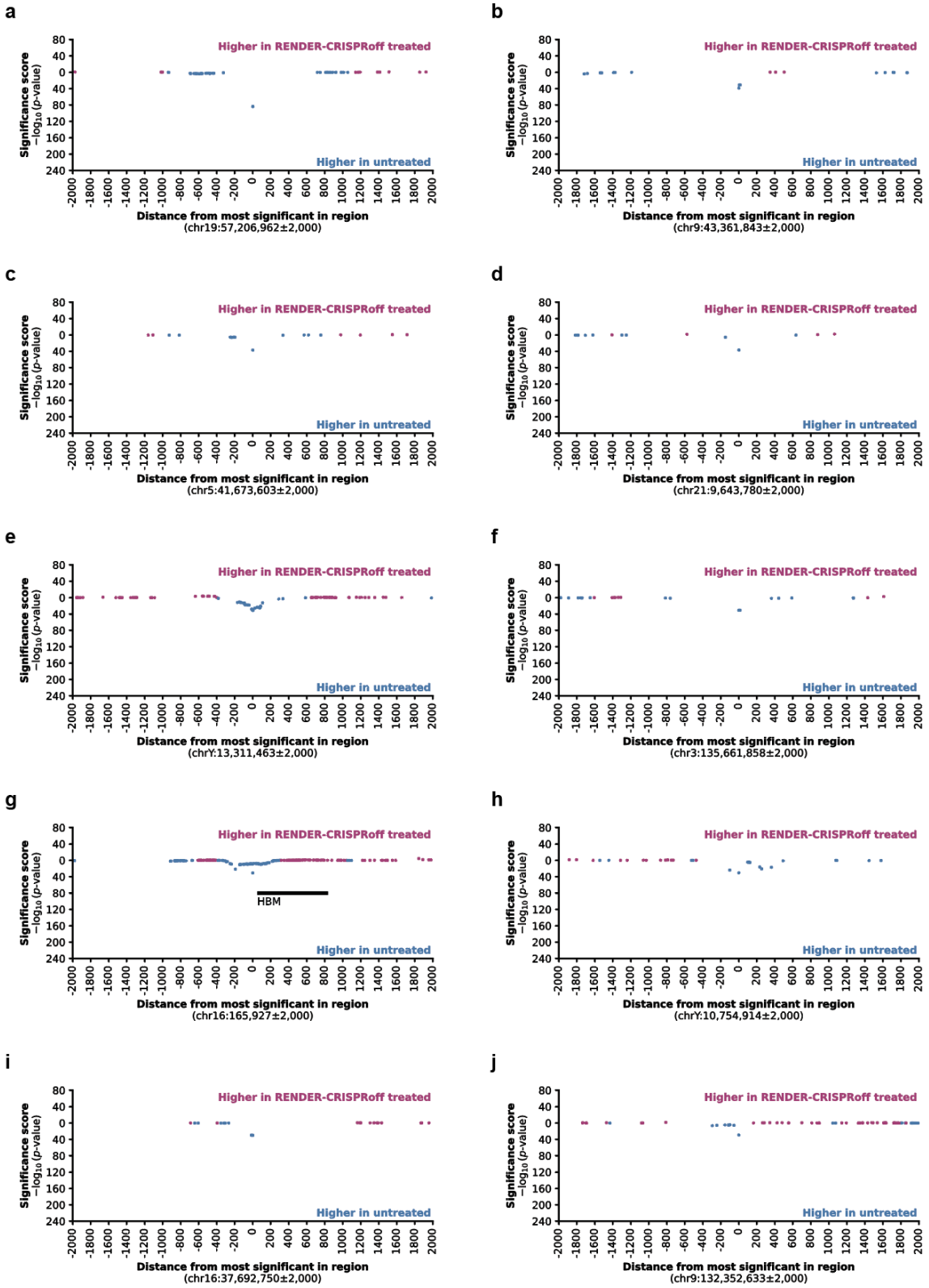

Extended Data Fig. 5: Analysis of decreased DNA methylation after RENDER-CRISPRoff treatment.

Extended Data Fig. 5a-j, Top ten most significant regions that are more methylated in untreated versus RENDER-CRISPRoff treated Jurkat cells, as analyzed by whole-genome EM-seq. Magenta dots represent CpGs that gained DNA methylation in RENDER-CRISPRoff-treated cells and blue dots represent CpGs that gained DNA methylation in untreated cells. Black bars denote genes.